

Exciton coherence-size and phonon-mediated optical nonlinearities in restricted geometries

Oleg Dubovsky and Shaul Mukamel

Department of Chemistry and Center For Photoinduced Charge Transfer, University of Rochester, Rochester, New York 14627

(Received 13 May 1991; accepted 25 July 1991)

The magnitude of optical nonlinearities of molecular nanostructures is determined by a characteristic *coherence-length* which controls the cooperativity of the optical response. Equations of motion describing the evolution of the optical polarization coupled to two-exciton variables are derived, and used to calculate the third order optical response ($\chi^{(3)}$) of a one-dimensional molecular crystal or a polymer. We show that the coherence-length is determined by the interplay between intramolecular and intermolecular (nonlocal) nonlinearities and explore the limitations of the local-field approximation. Phonon-mediated exciton-exciton attractive interaction may result in the formation of bound exciton pairs (biexcitons). We show how unbound (two-exciton) as well as biexciton states could readily be observed as resonances in two-photon absorption and third harmonic generation.

I. INTRODUCTION

Calculations of nonlinear optical response in condensed phases are usually based on a mean-field ansatz: the local-field approximation.¹⁻³ Underlying this approximation is the implicit assumption that the origin of the nonlinearity is *intramolecular*. The system may then be viewed as a collection of localized anharmonic oscillators with intermolecular *harmonic* dipole-dipole coupling. In this picture, the nonlinear susceptibilities assume the form of a product of a single molecule hyperpolarizability, times "local-field" corrections which account in a simple way for intermolecular interactions. This picture is greatly oversimplified. In reality, the optical response of molecular clusters, monolayers, and crystals is related to the dynamics of delocalized coherent excitations: the Frenkel excitons.⁴⁻⁶ The conventional local-field picture neglects the effects of the exciton coherence-size, which may result in enhanced nonlinearities.⁷⁻⁹ It also neglects any intermolecular nonlinearities resulting, e.g., from interactions among excitons, and possible biexciton formation.¹⁰ A close look at the limitations of the local-field picture and a systematic way for its generalization can be obtained using a microscopic approach based on equations of motion.^{11,12} A zero-temperature theory of nonlinear optical response which incorporates the effects of cooperative spontaneous emission (superradiance) was developed recently.¹² That theory showed how a cooperative enhancement of optical nonlinearities may be induced by the contribution of two-exciton states to the optical polarization. The effective zero-temperature coherence-size is equal to the optical wavelength. Intramolecular nonlinearities and their dependence on coupling with phonons at finite temperature were explored in a recent study of transient grating spectroscopy in molecular crystals.¹¹ Intermolecular coherences and their role in superradiance in molecular aggregates were investigated as well.¹³ A temperature-dependent coherence length which controls the magnitude of superradiance was calculated.

In this work we combine the methods of these earlier works^{11,12} to derive an expression for $\chi^{(3)}$ of one-dimensional molecular aggregates. Particular attention is paid to

the coherence-size and its dependence on exciton-phonon scattering. We show that phonon-mediated exciton pairing which is reminiscent of Cooper pairs in superconductivity¹⁴ may result in the formation of bound biexcitons with a large nonlinearity. The present model applies to molecular crystals¹⁵ as well as polymers such as polyacetylenes or polysilanes.¹⁶⁻¹⁹ An extension to other nanostructures such as monolayers^{20,21} is straightforward. In Sec. II we derive the equations of motion for the system, which include exciton and phonon variables. In Sec. III we present a formal solution for $\chi^{(3)}$ in terms of Green functions related to two-exciton and exciton-population variables. In Sec. IV we use a simplified model for phonon damping to solve for the Green functions, resulting in a closed form expression for $\chi^{(3)}$. In Sec. V we show how the nonlinear coherence size appears naturally in $\chi^{(3)}$. To this end, we factorize the intermolecular (nonlocal) nonlinearities into products of single-molecule variables when the two molecules are separated by M bonds or more. We thus retain the short-range (local) nonlinearities and neglect long-range nonlinearities. The factorization size M can then be varied at will. For $M = 1$ we recover the conventional local-field approximation. As M is increased, the nonlinear response eventually becomes M independent. The characteristic M value where this happens provides an operational definition of the *coherence-size* N_c . Numerical calculations of two-photon absorption and third harmonic generation, and a general discussion are presented in Sec. VI.

II. EQUATIONS OF MOTION

We consider a one-dimensional chain of N identical two-level molecules. The Hamiltonian consists of an electronic (exciton) term, a phonon term, an exciton-phonon interaction, and the interaction with the transverse electric field^{11,13}

$$H = H_{\text{ex}} + H_{\text{phon}} + H_{\text{ex-phon}} + H_{\text{ex-phot}}, \quad (2.1)$$

where

$$H_{ex} = \sum_n \hbar\Omega B_n^\dagger B_n + \sum_{n \neq m} \hbar J_{nm} (B_n + B_n^\dagger)(B_m + B_m^\dagger). \quad (2.2)$$

Here, B_n^\dagger are the exciton creation operators for the n th molecule, which satisfy the Pauli commutation rules

$$[B_n, B_m^\dagger] = (1 - 2B_n^\dagger B_n)\delta_{nm}. \quad (2.3)$$

J_{nm} is the dipole-dipole coupling between the m and n molecules.⁴ In k space we have

$$B_k = \frac{1}{\sqrt{N}} \sum_n B_n \exp(-ikn), \quad (2.4)$$

$$J_k = \sum_{n(\neq m)} J_{nm} \exp[ik(n-m)]. \quad (2.5)$$

The phonon part is

$$H_{phon} = \sum_q \hbar\omega_q b_q^\dagger b_q, \quad (2.6)$$

where b_q^\dagger is the Bose creation operator for the q phonon. These operators satisfy the commutation rules $[b_q, b_{q'}^\dagger] = \delta_{qq'}$. The exciton-phonon coupling is^{4,13}

$$H_{ex-phon} = \frac{1}{\sqrt{N}} \sum_{k,q} F_{k,q} B_{k+q}^\dagger B_k (b_q + b_{-q}^\dagger), \quad (2.7)$$

where F depends on the specific model.⁴ Denoting the transverse classical electric field by $E(k,t)$, we have for the coupling with the radiation field

$$H_{ex-photon} = -\frac{\sqrt{N}}{V} \sum_k \mu E(k,t) (B_k + B_{-k}^\dagger). \quad (2.8)$$

Here μ is the component of the molecular transition dipole matrix element which is parallel to the applied field. For clarity, and since we consider a one-dimensional model we shall not use a vector notation in this paper. It should be emphasized that although we are using here the terminology of a molecular crystal, the present model can be applied also to polymers such as polysilanes¹⁹ whose elementary excitations are Frenkel excitons.

The dynamics of the system will be calculated using the Heisenberg equations of motion for the dynamical variables responsible for the optical nonlinearity. The procedure was developed earlier,^{11,12} and the main steps are outlined in Appendices A and B. The resulting equations of motion which will be used in the calculation of the nonlinear susceptibility $\chi^{(3)}$ are

$$\begin{aligned} \frac{1}{i} \frac{d}{dt} \langle B_k \rangle = & - [\Omega + J_k + \Sigma(k)] \langle B_k \rangle - J_k \langle B_{-k}^\dagger \rangle + \frac{2}{N} \sum_{k',k''} J_{k'} [\langle B_{k''+k}^\dagger B_{k+k''} B_{k'} \rangle \\ & + \langle B_{k''+k}^\dagger B_{k+k''} B_{-k'}^\dagger \rangle] - (2\mu\rho N^{-3/2}/\hbar) \sum_{k'} E(k',t) \left(\sum_{k''} \langle B_{k'+k''}^\dagger B_{k+k''} \rangle - \frac{N}{2} \delta_{k,k'} \right), \end{aligned} \quad (2.9)$$

$$\begin{aligned} \frac{1}{i} \frac{d}{dt} \langle B_{k_1}^\dagger B_{k_2} \rangle = & [J_{k_1} + \Sigma^*(k_1) - J_{k_2} - \Sigma(k_2)] \langle B_{k_1}^\dagger B_{k_2} \rangle + \sum_q [\Sigma^*(k_2, k_1, q) - \Sigma(k_2, k_1, q)] \\ & \times \langle B_{k_1+q}^\dagger B_{k_2+q} \rangle + (\rho\mu N^{-1/2}/\hbar) [\langle B_{k_1}^\dagger \rangle E(k_2, t) - \langle B_{k_2} \rangle E(k_1, t)], \end{aligned} \quad (2.10)$$

$$\begin{aligned} \frac{1}{i} \frac{d}{dt} \langle B_{k_1} B_{k_2} \rangle = & - [2\Omega + J_{k_1} + \Sigma(k_1) + J_{k_2} + \Sigma(k_2)] \langle B_{k_1} B_{k_2} \rangle + \sum_q [\Sigma'(k_1, k_2, q) \\ & + \Sigma'(k_2, k_1, -q)] \langle B_{k_2-q} B_{k_1+q} \rangle + (\rho\mu N^{-1/2}/\hbar) [\langle B_{k_1} \rangle E(k_2, t) + \langle B_{k_2} \rangle E(k_1, t)], \end{aligned} \quad (2.11)$$

where $\langle \dots \rangle$ denotes an expectation value, and

$$\begin{aligned} \langle B_{k''+k}^\dagger B_{k+k''} B_{k'} \rangle = & \langle B_{k''+k}^\dagger B_{k+k''} \rangle \langle B_{k'} \rangle + \langle B_{k''+k}^\dagger B_{k'} \rangle \langle B_{k+k''} \rangle \\ & + \langle B_{k''+k}^\dagger \rangle \langle B_{k+k''} B_{k'} \rangle - 2 \langle B_{k''+k}^\dagger \rangle \langle B_{k+k''} \rangle \langle B_{k'} \rangle. \end{aligned} \quad (2.12)$$

A similar factorization holds also for the other three-operator variable by replacing $B_{k'}$ in Eq. (2.12) by $B_{-k'}^\dagger$. In Eqs. (2.9)–(2.12), all B_k (B_k^\dagger) operators are Heisenberg operators at time t , $\rho \equiv N/V$ is the molecular density, and $E(k,t)$ is the Fourier component of the electric field. The phonon-induced self-energies are given by¹¹

$$\begin{aligned} \Sigma(k, k', q) = & \frac{1}{\hbar^2 N} \lim_{\eta \rightarrow +0} F_{k,q}^* F_{k',q} \\ & \times \left(\frac{n_q}{J_{k'+q} - J_{k'} - \omega_q - i\eta} \right. \\ & \left. + \frac{1+n_{-q}}{J_{k'+q} - J_{k'} + \omega_{-q} - i\eta} \right), \end{aligned} \quad (2.13)$$

$$\Sigma(k) \equiv - \sum_q \Sigma(k, k, q) - i(\gamma/2), \quad (2.14)$$

and

$$\begin{aligned} \Sigma'(k, k', q) = & \frac{1}{\hbar^2 N} \lim_{\eta \rightarrow +0} F_{k,q}^* F_{k',-q}^* \\ & \times \left(\frac{n_q}{J_{k'} - J_{k'-q} - \omega_q - i\eta} \right. \\ & \left. + \frac{1+n_{-q}}{J_{k'} - J_{k'-q} + \omega_q - i\eta} \right), \end{aligned} \quad (2.15)$$

with the boson thermal occupation number

$$n_q \equiv \frac{1}{[\exp(\hbar\omega_q/kT)] - 1}. \quad (2.16)$$

The self-energies Σ and Σ' are in general complex. The real part represents level shifts wherever the imaginary part represents relaxation and damping. In Eq. (2.14) we have included an additional damping rate γ which represents the exciton lifetime.

Equations (2.9)–(2.12) were derived as follows. The Heisenberg equations obtained using the Hamiltonian (2.1) result in an infinite hierarchy of equations which successively couple B and B^\dagger to higher operators containing products of more B and B^\dagger operators. This hierarchy may be truncated at the cubic level,^{11,12} and operators containing products of four or more B or B^\dagger operators need not be considered, since their expectation values are at least fourth order in the E field, and they do not contribute to $\chi^{(3)}$. This results in the equations of motion given in Appendix A. The calculation of higher order susceptibilities such as $\chi^{(5)}$ will, of course, require the generalization of these equations by adding more dynamical variables.²² The factorization (2.12) of the triple product of operators, which is derived in Appendix B allows us to close the hierarchy at the quadratic (two-operator) level. It is based on an ansatz for the density matrix [Eq. (B1)] which can be rationalized using maximum entropy arguments. Finally, the phonon variables are eliminated using the procedure given in Appendix A of Ref. 11, resulting in Eqs. (2.9)–(2.16). These equations contain three types of variables: $\langle B_k \rangle$ represent the exciton amplitudes which determine the optical polarization [Eq. (3.3)], $\langle B_{k_1}^\dagger B_{k_2} \rangle$ represent exciton populations (EP) and $\langle B_{k_1} B_{k_2} \rangle$ represent two-exciton (TE) variables. The interaction with phonons is incorporated by calculating a self-energy which is evaluated to second order in the exciton–phonon coupling. Two self-energy terms appear in the present theory: Σ for the EP variables and Σ' for the TE variables.

Equations (2.9)–(2.12) form the basis for the theory developed in this article. They map the problem of calculating optical nonlinearities onto the dynamics of a coupled set of anharmonic oscillators. This is a natural extension of the harmonic oscillator (Drude) picture of linear optics.^{23,24} An anharmonic oscillator picture is frequently used in qualitative descriptions of the nonlinear optical response.¹ The present derivation provides a rigorous and a systematic method for identifying the oscillators in terms of single-particle and two-particle dynamical variables.

III. GREEN FUNCTION EXPRESSIONS FOR OPTICAL SUSCEPTIBILITIES

In a four wave mixing experiment, the system is interacting with three light waves. The electric field is then given by¹

$$E(r,t) = \sum_{j=1}^3 E_j \exp(-ik_j r + i\omega_j t) + \text{c.c.} \quad (3.1)$$

We shall consider a stationary (frequency-domain) experiment where the field amplitudes E_j do not depend on time. E_j and the field amplitude introduced in Eq. (2.8) are related by

$$E(k_j, t) = V E_j \exp(-i\omega_j t), \quad (3.2)$$

with V being the quantization volume. The linear and the nonlinear optical response is expressed in terms of the expectation value of the optical polarization, defined by

$$P(k) = \sqrt{N} \mu (\langle B_k \rangle + \langle B_{-k}^\dagger \rangle). \quad (3.3a)$$

In analogy with Eq. (3.1) we introduce the polarization amplitude

$$P(r,t) = \sum_j P_j \exp(-ik_j r + i\omega_j t) + \text{c.c.}, \quad (3.3b)$$

so that

$$P(k_j, t) = V P_j \exp(-i\omega_j t). \quad (3.3c)$$

In order to calculate the optical susceptibilities, we need to solve the coupled equations of motion for the P , EP, and TE variables. This could be done by expanding all variables in a power series in the electric field, and solving for successively higher orders. The optical polarization is then given by a series $P_j = P_j^{(1)} + P_j^{(2)} + \dots$, where the superscripts denote an order with respect to the field amplitudes E_j . In all the calculations reported below, we have further invoked the rotating wave approximation, thereby neglecting off-resonant contributions to the nonlinear response. This amounts to neglecting the $\langle B_{-k}^\dagger \rangle$ and the $\langle B_{k'+k}^\dagger B_{k+k'} B_{-k}^\dagger \rangle$ terms on the right hand side of Eq. (2.9). Consider first the linear response. When Eq. (2.9) is linearized we get

$$\frac{1}{i} \frac{d}{dt} \langle B_{k_j} \rangle^{(1)} = - [\Omega + J_{k_j} + \Sigma(k_j)] \langle B_{k_j} \rangle^{(1)} + \frac{(\rho\mu/\hbar)}{\sqrt{N}} E(k_j, t). \quad (3.4)$$

The steady state solution of Eq. (3.4) can be obtained using the substitution

$$\langle B_{k_j} \rangle^{(1)} = \frac{V}{\sqrt{N}} \frac{1}{\mu} \exp(-i\omega_j t) \chi^{(1)}(k_j, \omega_j) E_j, \quad (3.5)$$

where the linear susceptibility is defined by

$$P_j^{(1)} = \chi^{(1)}(k_j, \omega_j) E_j. \quad (3.6)$$

Equations (3.4)–(3.6) result in

$$\chi^{(1)}(k_j, \omega_j) = - \frac{(\rho/\hbar)\mu^2}{\omega_j - \Omega - J_{k_j} - \Sigma(k_j)}. \quad (3.7)$$

This is the conventional expression for the linear susceptibility.^{4,11}

We next turn to the nonlinear response. For the present model $P_j^{(2)} = 0$ so that the lowest order nonlinear polarization is

$$P^{(3)}(k_s) = \mu\sqrt{N} [\langle B_{k_s} \rangle^{(3)} + \langle B_{-k_s}^\dagger \rangle^{(3)}]. \quad (3.8)$$

In general, k_s can be any combination of the form $k_s = \pm k_1 \pm k_2 \pm k_3$. Hereafter we choose $k_s = k_1 - k_2 + k_3$ and $\omega_s = \omega_1 - \omega_2 + \omega_3$. Any other combination may be obtained from our final expression by changing ω_j , k_j , and E_j to $-\omega_j$, $-k_j$, and E_j^* , respectively. With our choice of k_s , we shall calculate the nonlinear susceptibility

$$P_s^{(3)} = \chi^{(3)}(-k_s, -\omega_s; k_1, \omega_1, -k_2, -\omega_2, k_3, \omega_3) E_1 E_2^* E_3. \quad (3.9)$$

In order to calculate $P_s^{(3)}$, we first solve Eq. (2.10) for the EP variables, with the substitution of Eq. (3.5) in the right-hand side. These variables are second order in the field. We define the solution of Eq. (2.10) by introducing a Green function $G_{k_2k_1}(q)$ for the EP variables¹¹

$$\langle B_{k_2+q}^\dagger B_{k_1+q} \rangle \equiv \frac{V^2}{N} G_{k_2k_1}(q) E_1 E_2^* \exp[i(\omega_2 - \omega_1)t]. \tag{3.10}$$

Upon the substitution of Eq. (3.10) in Eq. (2.10) and transforming to ω space, we obtain the following equation for the Green function:

$$\begin{aligned} [\omega_2 - \omega_1 - \epsilon^*(k_2 + q) + \epsilon(k_1 + q)] G_{k_2k_1}(q) \\ = - \sum_{q'} \Sigma_{k_2k_1}^{(1)}(q, q') G_{k_2k_1}(q' + q) \\ - (\rho/\hbar) [\chi^{(1)}(k_1, \omega_1) - \chi^{(1)}(k_2, \omega_2)] \delta_{q,0}, \end{aligned} \tag{3.11a}$$

where the self-energy $\Sigma^{(1)}$ is defined as

$$\Sigma_{k_2k_1}^{(1)}(q, q') \equiv \Sigma^*(k_2 + q, k_1 + q, q') - \Sigma(k_1 + q, k_2 + q, q'), \tag{3.11b}$$

and

$$\epsilon(k) \equiv \Omega + J_k + \Sigma(k). \tag{3.12}$$

Throughout this article the q and q' summations run over the values $2\pi p/N$ with $p = 0, \dots, N - 1$. We next repeat the same procedure for the TE variables.¹² In analogy with Eq. (3.10) we introduce the corresponding Green function $D_{k_1k_3}(q)$,

$$\langle B_{k_1+q} B_{k_3-q} \rangle \equiv \frac{V^2}{N} D_{k_1k_3}(q) E_1 E_3 \exp[-i(\omega_1 + \omega_3)t]. \tag{3.13}$$

Replacing $\langle B \rangle$ in the right-hand side of Eq. (2.11) by $\langle B \rangle^{(1)}$, and substituting Eq. (3.13), we obtain the following equations for the TE Green function:

$$\begin{aligned} [\omega_1 + \omega_3 - \epsilon(k_1 + q) - \epsilon(k_3 - q)] D_{k_1k_3}(q) \\ = \sum_{q'} \Sigma_{k_1k_3}^{(2)}(q, q') D_{k_1k_3}(q' + q) \\ - (\rho/\hbar) [\chi^{(1)}(k_1, \omega_1) + \chi^{(1)}(k_3, \omega_3)] \delta_{q,0}, \end{aligned} \tag{3.14a}$$

with the corresponding self-energy

$$\begin{aligned} \Sigma_{k_1k_3}^{(2)}(q, q') \equiv \Sigma'(k_1 + q, k_3 - q, q') \\ + \Sigma'(k_3 - q, k_1 + q, q'). \end{aligned} \tag{3.14b}$$

We now turn to the calculation of $\langle B \rangle^{(3)}$. Upon the substitution of Eqs. (3.10) and (3.13) in Eq. (2.9) and collecting terms to third order in the field, we obtain

$$\begin{aligned} \frac{1}{i} \frac{d}{dt} \langle B_{k_s} \rangle^{(3)} = - [\Omega + J_{k_s} + \Sigma(k_s)] \langle B_{k_s} \rangle^{(3)} + \frac{2V^3}{N^2 \sqrt{N} \mu} \sum_p E_2^* E_1 E_3 \\ \times \left[\chi^{(1)}(k_3, \omega_3) J_{k_3} \sum_q G_{k_2k_1}(q) + \chi^{(1)}(k_3, \omega_3) \sum_q J_{q+k_1} G_{k_2k_1}(q) + \chi^{(1)*}(k_2, \omega_2) \sum_q J_{k_1+q} D_{k_1k_3}(q) \right. \\ \left. - 2J_{k_3} \chi^{(1)*}(k_2, \omega_2) \chi^{(1)}(k_1, \omega_1) \chi^{(1)}(k_3, \omega_3) - (\rho/\hbar) \mu^2 \sum_q G_{k_2k_1}(q) \right], \end{aligned} \tag{3.15}$$

where Σ_p stands for a sum over the six permutations of the fields (k_1, ω_1 , $-k_2 - \omega_2$, and k_3, ω_3). This sum accounts for all possible time-orderings of the various interactions. Solving for the third order polarization Eq. (3.8) and using Eq. (3.9) we finally obtain for the third order susceptibility

$$\begin{aligned} \chi^{(3)}(-k_s - \omega_s; k_1, \omega_1, -k_2 - \omega_2, k_3, \omega_3) \\ = \frac{2V^2}{N^2} \frac{1}{[-\omega_s + \Omega + J_{k_s} + \Sigma(k_s)]} \sum_p \left[-2J_{k_3} \mu^{-2} \chi^{(1)*}(k_2, \omega_2) \chi^{(1)}(k_1, \omega_1) \chi^{(1)}(k_3, \omega_3) - (\rho/\hbar) \mu^2 \sum_q G_{k_2k_1}(q) \right. \\ \left. + \chi^{(1)}(k_3, \omega_3) J_{k_3} \sum_q G_{k_2k_1}(q) + \chi^{(1)}(k_3, \omega_3) \sum_q J_{k_1+q} G_{k_2k_1}(q) + \chi^{(1)*}(k_2, \omega_2) \sum_q J_{k_1+q} D_{k_1k_3}(q) \right]. \end{aligned} \tag{3.16}$$

Equation (3.16) provides a closed formal expression for $\chi^{(3)}$ in terms of the Green functions for the EP and TE variables (G and D , respectively). It contains three types of terms. The first term in the square brackets represents the contribution of the cubic nonlinearity (CN) $\langle B^\dagger \rangle \langle B \rangle \langle B \rangle$ in the equation of motion. The following three terms which contain the Green function G represent the contribution of the $\langle B^\dagger B \rangle \langle B \rangle$ exciton-population nonlinearity, and the last term with the Green function D represents the contribution of the two-exciton $\langle B^\dagger \rangle \langle BB \rangle$ nonlinearity.

A simple limit is provided by the single-particle approximation,¹¹ where we factorize the expectation values of all products of operators into the products of expectation val-

ues, thus retaining only single-particle variables, i.e.,

$$\langle B_{k_2}^\dagger B_{k_1} \rangle \cong \langle B_{k_2}^\dagger \rangle \langle B_{k_1} \rangle, \tag{3.17}$$

$$\langle B_{k_1} B_{k_3} \rangle \cong \langle B_{k_1} \rangle \langle B_{k_3} \rangle. \tag{3.18}$$

We thus get

$$G_{k_2k_1}(q) = \frac{1}{\mu^2} \chi^{(1)*}(k_2, \omega_2) \chi^{(1)}(k_1, \omega_1) \delta_{q,0}, \tag{3.19}$$

$$D_{k_1k_3}(q) = \frac{1}{\mu^2} \chi^{(1)}(k_3, \omega_3) \chi^{(1)}(k_1, \omega_1) \delta_{q,0}, \tag{3.20}$$

and

$$\frac{1}{i} \frac{d}{dt} \langle B_{k_s} \rangle^{(3)} = - [\Omega + J_{k_s} + \Sigma(k_s)] \langle B_{k_s} \rangle^{(3)} + \frac{2\sqrt{N}}{\mu^3 \rho^3} \sum_{\mathbf{p}} \delta_{k_s, k_1 - k_2 + k_3} [\omega_1 - \Omega - \Sigma(k_1)] \times \chi^{*(1)}(k_2, \omega_2) \chi^{(1)}(k_1, \omega_1) \chi^{(1)}(k_3, \omega_3) E_2^* E_1 E_3. \quad (3.21)$$

Upon the substitution of Eqs. (3.7), (3.19), and (3.20) in Eq. (3.16) we get^{2,11}

$$\chi^{(3)}(-k_s - \omega_s; k_1, \omega_1, -k_2 - \omega_2, k_3, \omega_3) = \frac{2\rho\mu^4}{\hbar^2} \sum_{\mathbf{F}} \frac{[\omega_1 - \Omega - \Sigma(k_1)]}{[\omega_s - \Omega - J_{k_s} - \Sigma^*(k_s)] \times [\omega_2 - \Omega - J_{k_2} - \Sigma^*(k_2)] [\omega_1 - \Omega - J_{k_1} - \Sigma(k_1)] [\omega_3 - \Omega - J_{k_3} - \Sigma(k_3)]}. \quad (3.22)$$

In the next section we shall introduce a simplified model for the exciton-phonon coupling, which will allow us to solve Eqs. (3.11a) and (3.14a) for the necessary Green functions and obtain an explicit expression for $\chi^{(3)}$ which goes beyond the single-particle approximation, Eq. (3.22).

IV. FOUR-WAVE MIXING AND $\chi^{(3)}$

We now adopt the following simplified model for the exciton-phonon coupling:

$$H_{\text{ex-phon}} = \frac{1}{2} F_0 \sum_n B_n^\dagger B_n (b_n + b_n^\dagger), \quad (4.1)$$

where the phonon annihilation operator in real space is

$$b_n = \frac{1}{\sqrt{N}} \sum_q b_q \exp(iqn). \quad (4.2)$$

Equation (4.1) represents a site-diagonal coupling to optical phonons. Transforming to k space yields Eq. (2.7) with

$$F_{k,q} = F_0. \quad (4.3)$$

Using Eq. (4.3) we obtain from Eq. (2.13) for the self-energy for the EP variables¹¹

$$\Sigma_{k_1, k_1}^{(1)}(q, q') = i \frac{\Gamma}{N} - i(\Gamma + \gamma) \delta_{q,0}, \quad (4.4)$$

and the exciton damping is

$$\Sigma(k) = -i(\Gamma + \gamma)/2, \quad (4.5)$$

where γ^{-1} is the exciton lifetime, and

$$\Gamma = \frac{2|F_0|^2}{\hbar^2} n_q \text{Im} \left[\frac{1}{J_q - J_0 - \omega_q - i\eta} + \frac{1}{J_q - J_0 + \omega_q - i\eta} \right], \quad (4.6)$$

where \mathbf{q} is a typical average wave vector. Equation (4.4) represents a *strong-collision* model, where each k exciton is scattered to all other k' excitons with the same rate Γ/N . Correspondingly, at long times, all exciton states will be equally populated. This relaxation thus corresponds to an *infinite-temperature* damping mechanism, known as the Haken-Ströbl model. It was recently applied to transient-grating spectroscopy.¹¹

We next turn to calculating the self-energy of the two-exciton variables $\Sigma^{(2)}$. To that end we adopt the following simplified model for the exciton-phonon coupling:

$$H_{\text{ex-phon}} = \frac{1}{2} F'_0 \sum_{nm} B_n^\dagger B_m (b_n + b_m) (\delta_{n,m+1} + \delta_{n,m-1}) + \text{h.c.} \quad (4.7)$$

Equation (4.7) represents an off-diagonal coupling with acoustic phonons. Upon transforming to k space we have

$$H_{\text{ex-phon}} = \sum_{nmp} F'_0 B_n^\dagger B_m b_p \left(\frac{1}{2N^2} \sum_{k,q} [\cos(k+q) + \cos(k)] \exp\{i[(k+q)n - km - qp]\} \right) + \text{h.c.}, \quad (4.8)$$

which finally yields Eq. (2.7) with

$$F_{k,q} = F'_0 \cos[k + (q/2)] \cos(q/2). \quad (4.9)$$

Using Eq. (4.9) we get

$$F_{k_1, q} F_{k_3, -q} = \frac{1}{2} F_0'^2 [\cos(k_1 + k_3) + \cos(k_1 - k_3 + q)] \times [1 + \cos(q)]. \quad (4.10)$$

We shall maintain the essential q dependence of the product and replace it by

$$F_{k_1, q} F_{k_3, -q} \cong \frac{1}{2} F_0'^2 [\cos(k_1 - k_3 + q) + \cos(q)]. \quad (4.11)$$

Proceeding along similar lines to those leading to $\Sigma^{(1)}$ we obtain

$$\Sigma_{k_1, k_3}^{(2)}(q, q') = -\frac{\Gamma_0}{N} \cos\left(q + \frac{k_1 - k_3}{2}\right) \cos\left(q + q' + \frac{k_1 - k_3}{2}\right), \quad (4.12)$$

where

$$\Gamma_0 = \frac{2F_0'^2 n_q}{\hbar^2} \left[\frac{1}{J_0 - J_q - \omega_q - i\eta} + \frac{1}{J_0 - J_q + \omega_q - i\eta} \right] \equiv \Gamma_0' + i\Gamma_0''. \quad (4.13)$$

Here Γ_0' and Γ_0'' are the real and imaginary parts, respectively, of the $\Sigma^{(2)}$ kernel.

The relaxation kernels given by Eqs. (4.4), (4.5), and (4.12) will be used in the following calculations. An alternative simplified way of deriving these forms of the relaxation kernels is by using a stochastic model for the exciton-phonon coupling

$$H_{\text{ex-phon}} = \hbar \sum_n \delta\Omega_n(t) B_n^\dagger B_n. \quad (4.14)$$

$\delta\Omega_n(t)$ is a stochastic Gaussian random variable with the following properties:

$$\langle \delta\Omega_n(t) \rangle = 0, \quad (4.15)$$

$$i \langle \delta\Omega_n(t) \delta\Omega_m(t') \rangle$$

$$= \begin{cases} i \frac{\Gamma}{2} \delta(t-t') & n = m \\ \frac{1}{4} (\Gamma'_0 + i\Gamma''_0) \delta(t-t') & n = m \pm 1 \\ 0 & \text{else} \end{cases} \quad (4.16)$$

Using this model, we obtain the following relaxation terms in the equations of motion:

$$\left[\frac{d}{dt} \langle B_n(t) \rangle \right]_{\text{phon}} = -\frac{\tilde{\Gamma}}{2} \langle B_n(t) \rangle. \quad (4.17a)$$

$$\left[\frac{d}{dt} \langle B_n^\dagger(t) B_m(t) \rangle \right]_{\text{phon}} = -[\Gamma(1 - \delta_{nm}) + \gamma] \langle B_n^\dagger(t) B_m(t) \rangle, \quad (4.17b)$$

$$\left[\frac{d}{dt} \langle B_n(t) B_{n\pm 1}(t) \rangle \right]_{\text{phon}} = \frac{i}{4} (\Gamma'_0 + i\Gamma''_0) \langle B_n(t) B_{n\pm 1}(t) \rangle. \quad (4.17c)$$

Equations (4.17a) and (4.17b) represent the Haken–Ströbl model of exciton relaxation.^{11,25} By transforming to k space, Eqs. (4.17) will result in the relaxation terms given by Eqs. (4.4), (4.5), and (4.12). The real-space representation of the relaxation [Eqs. (4.17)] will be used in the next section.

In order to obtain a simple closed form expression for $\chi^{(3)}$, we further approximate the dipolar coupling by a nearest-neighbor coupling $J_{nm} = V\delta_{n,m\pm 1}$ which gives $J_k = 2V \cos k$. In Appendix C we calculate the Green functions G and D [Eqs. (3.11) and (3.14)] using the self-energies Eqs. (4.4) and (4.12). Using these Green functions we finally obtain for $\chi^{(3)}$ of an infinite crystal ($N \rightarrow \infty$)

$$\begin{aligned} \chi^{(3)}(-k_s - \omega_s; k_1 \omega_1, -k_2 - \omega_2, k_3 \omega_3) &= \frac{2\rho\mu^4}{\hbar^3} \sum_p \frac{1}{(\omega_s - \Omega - J_{k_s} + i\frac{\tilde{\Gamma}}{2})(\omega_2 - \Omega - J_{k_2} + i\frac{\tilde{\Gamma}}{2})(\omega_1 - \Omega - J_{k_1} + i\frac{\tilde{\Gamma}}{2})(\omega_3 - \Omega - J_{k_3} + i\frac{\tilde{\Gamma}}{2})} \\ &\times \left\{ (\omega_1 - \Omega - J_{k_1} + i\frac{\tilde{\Gamma}}{2}) \phi(k_1, k_2) - i\Gamma \phi(k_1, k_2) \left[\frac{J_{k_3}}{(\omega_2 - \omega_1 - i\tilde{\Gamma})I(k_1, k_2)} + (J_{k_2} - J_{k_1}) \psi(k_1, k_2) \right] \right. \\ &\left. + \frac{1}{2} \frac{(J_{k_1} + J_{k_3})}{[1 - \Gamma_0 \kappa(k_s + k_2)]} \right\}, \quad (4.18) \end{aligned}$$

where we have introduced the following auxiliary functions:

$$\phi(k_1, k_2) \equiv 1 / \left[1 + i \frac{\Gamma}{(\omega_2 - \omega_1 - i\tilde{\Gamma})I(k_1, k_2)} \right], \quad (4.19)$$

$$\tilde{\Gamma} \equiv \Gamma + \gamma, \quad (4.20)$$

$$I(k_1, k_2) \equiv \sqrt{1 - \left[\frac{4V \sin[(k_1 - k_2)/2]}{\omega_2 - \omega_1 - i\tilde{\Gamma}} \right]^2}, \quad (4.21)$$

$$\psi(k_1, k_2) \equiv \frac{1}{2} \frac{\{1 - [I(k_1, k_2)]^{-1}\}}{(J_{k_2} - J_{k_1})}, \quad (4.22)$$

$$\kappa(k_s + k_2)$$

$$\equiv \frac{1}{(\omega_3 + \omega_1 - 2\Omega + i\tilde{\Gamma})} \frac{1}{\eta^2} \left(-1 + \frac{1}{\sqrt{1 - \eta^2}} \right), \quad (4.23)$$

with

$$\eta = 4V \cos[(k_s + k_2)/2] / (\omega_3 + \omega_1 - 2\Omega + i\tilde{\Gamma}). \quad (4.24)$$

Equation (4.18) has three terms in the curly brackets. They correspond, respectively, to the CN, EP, and TE nonlinearities which appear in Eq. (3.16). When expanded in powers of molecular density (and noting the additional overall ρ prefactor), we find that the first term gives a contribution $\sim \rho$, whereas the second (EP) and the third (TE) terms are $\sim \rho^2$. This is to be expected since the first term is due to

intramolecular (local) nonlinearity, whereas the other two are induced by intermolecular (nonlocal) interactions. Intermolecular interactions enter therefore Eq. (4.18) in two ways. They modify the intramolecular term, and they induce additional new terms. The appearance and the form of these new terms provide an excellent direct probe for intermolecular interactions, as will be demonstrated in Sec. VI.

V. THE LOCAL-FIELD APPROXIMATION: NONLINEAR COHERENCE-SIZE

The expression for $\chi^{(3)}$ derived in Sec. IV contains the contribution from intramolecular as well as intermolecular nonlinearities. The intermolecular nonlinearity results in the second and the third term in the curly brackets in Eq. (4.18). The third term may be responsible for an enhanced (cooperative) nonlinear optical response. The enhancement can most conveniently be described in terms of an exciton coherence length which represents the separation of two sites which can still respond coherently to the applied fields. In order to define the coherence-size more precisely and gain a clear insight into its role, we recast our equations of motion in real space. Eq. (A2) (without the phonon part) thus assumes the form

$$\begin{aligned} \frac{1}{i} \frac{d}{dt} B_n &= -\Omega B_n - \sum_m J_{nm} (B_m + B_m^\dagger) \\ &+ 2 \sum_m J_{nm} (B_n^\dagger B_n B_m + B_n^\dagger B_n B_m^\dagger) \\ &+ (\mu/\hbar) E(n) [1 - 2B_n^\dagger B_n]. \end{aligned} \quad (5.1)$$

The key approximation will now be introduced. The cubic variables $B_n^\dagger B_n B_m$ represent *coherences among the n and the m sites*, which contribute to the optical nonlinearity. If we assume the existence of a finite nonlinear coherence-size N_c in the problem, then the expectation values of these cubic terms can be factorized into a product of two single-particle factors when the n and m sites are separated by a number of bonds larger than N_c . In the equation of motion we thus retain the cubic variables if the two sites are separated by less than M bonds, and factorize them into products of single-site variables otherwise. M is an arbitrary chosen number which can be varied at will. We thus set

$$\begin{aligned} \langle B_n^\dagger B_n B_m \rangle &= \langle B_n^\dagger B_n \rangle \langle B_m \rangle, \quad |n-m| \geq M, \quad (5.2) \\ \langle B_n^\dagger B_n B_m \rangle &= \langle B_n^\dagger B_n \rangle \langle B_m \rangle + \langle B_n^\dagger B_m \rangle \langle B_n \rangle \\ &+ \langle B_n^\dagger \rangle \langle B_n B_m \rangle - 2 \langle B_n^\dagger \rangle \langle B_n \rangle \langle B_m \rangle, \\ &|n-m| < M. \end{aligned} \quad (5.3)$$

We expect the factorization made in Eq. (5.2) to be a serious approximation which will strongly affect $\chi^{(3)}$ as long as $M < N_c$. However, for $M > N_c$ this approximation should have a negligible effect, since the neglected coherences are not relevant anyhow. By varying M , and observing the variation of the calculated $\chi^{(3)}$ with M , we expect a saturation as M crosses over N_c . *This should confirm our ansatz regarding the existence of N_c , and provide an operational definition for N_c .*

Using Eq. (5.2), Eqs. (2.9), (2.10), and Eq. (2.11) now become

$$\begin{aligned} \frac{1}{i} \frac{d}{dt} \langle B_n \rangle &= -\left(\Omega - i \frac{\Gamma}{2}\right) \langle B_n \rangle - \sum_m J'_{nm} (\langle B_m \rangle) \\ &+ \langle B_m^\dagger \rangle - 2 \langle B_n^\dagger B_n B_m \rangle - 2 \langle B_n^\dagger B_n B_m^\dagger \rangle \\ &- (\mu/\hbar) E_n^l (2 \langle B_n^\dagger B_n \rangle - 1), \end{aligned} \quad (5.4)$$

$$\begin{aligned} \frac{1}{i} \frac{d}{dt} \langle B_n^\dagger B_m \rangle &= \sum_{m'} J'_{nm'} \langle B_{m'}^\dagger B_m \rangle - \sum_{m'} J'_{mm'} \langle B_n^\dagger B_{m'} \rangle \\ &+ i[\Gamma(1 - \delta_{nm}) + \gamma] \langle B_n^\dagger B_m \rangle \\ &+ (\mu/\hbar) (E_m^l \langle B_n^\dagger \rangle - E_n^l \langle B_m \rangle), \end{aligned} \quad (5.5)$$

$$\begin{aligned} \frac{1}{i} \frac{d}{dt} \langle B_n B_m \rangle &= -2\Omega \langle B_n B_m \rangle - \sum_{m'} J'_{nm'} \langle B_{m'} B_m \rangle \\ &- \sum_{m'} J'_{mm'} \langle B_n B_{m'} \rangle \\ &+ i\gamma \langle B_n B_m \rangle + i \frac{\Gamma_0}{4} \langle B_n B_m \rangle \delta_{n,m \pm 1} \\ &+ (\mu/\hbar) (E_m^l \langle B_n \rangle + E_n^l \langle B_m \rangle), \end{aligned} \quad (5.6)$$

where we have separated J_{nm} into a short-range (J'_{nm}) and a long-range part (J''_{nm})

$$J_{nm} \equiv J'_{nm} + J''_{nm},$$

with

$$J'_{nm} = \begin{cases} J_{nm}; & |n-m| < M \\ 0; & |n-m| \geq M \end{cases}, \quad (5.7a)$$

and

$$J''_{nm} = \begin{cases} 0; & |n-m| < M \\ J_{nm}; & |n-m| \geq M \end{cases}. \quad (5.7b)$$

We have further introduced the local-field at site n generated by the long-range part of the intermolecular interactions. This field is different from the average Maxwell field $E(n)$,

$$E_n^l \equiv E(n) - \frac{\hbar}{\mu} \sum_m J''_{nm} (\langle B_m \rangle + \langle B_m^\dagger \rangle). \quad (5.8)$$

We note that the factorization [Eq. (5.2)] has not affected Eqs. (5.5) and (5.6) which are identical to Eqs. (2.10) and (2.11), respectively. The partial neglect of nonlinearities only affected Eq. (5.4) which constitutes an approximation to Eq. (2.9). Equations (5.3)–(5.6) constitute a closed set of equations for single site variables $\langle B_n \rangle$, and two-site variables $\langle B_n B_m \rangle$ and $\langle B_n^\dagger B_m \rangle$ with $|n-m| < M$, and their complex conjugates. They have a simple physical interpretation. Intermolecular variables representing molecules separated by less than M bonds constitute nonlinear oscillators which are relevant for the optical nonlinearities. Long-range interactions among molecules whose separation is greater than M take place only via the local-field which is the field at site n generated by the average field and the contributions of the long-range interactions. Equations (5.2)–(5.6) provide a flexible prescription for calculating the nonlinear response. They offer a rigorous treatment of short-range dynamics and an approximate treatment of long-range interactions. The physical picture is that the system behaves as a collection of anharmonic oscillators. The anharmonicities are short-range, interactions among well-separated oscillators are harmonic! By choosing $M = 1$ we put all intermolecular interactions in the local-field; and as will be shown below, this results in the conventional local-field approximation.^{1,11} As M is increased, we treat the intermolecular interactions more rigorously, and the local field becomes closer to the average field. For $M = N$ we treat all intermolecular interactions explicitly, $E_n^l = E(n)$ and Eqs. (5.4)–(5.6) become identical to Eqs. (2.9)–(2.11). This interplay among local-field and intermolecular interactions has been discussed by Mukamel, Deng, and Grad.^{3(a)}

Equations (5.4)–(5.6) can be solved in a similar manner to what we did in Sec. IV. In this section we retain the general form of J_k and unlike Sec. IV we do not make a nearest-neighbor approximation. We further invoke the rotating wave approximation and neglect terms with off resonant denominators. The local-field is then given by

$$E^l(k, \omega) = \frac{\omega - \Omega - J'_k + i(\Gamma/2)}{\omega - \Omega - J_k + i(\Gamma/2)} E(k, \omega), \quad (5.9a)$$

with

$$J'_k = \sum_m J'_{mn} \exp[ik(n-m)] \quad (5.9b)$$

and similarly for J''_k . We finally obtain the M -dependent nonlinear susceptibility

$$\begin{aligned} \chi_M^{(3)}(-k_s - \omega_s, k_1, \omega_1, -k_2 - \omega_2, k_3, \omega_3) &= \frac{2\rho\mu^4}{\hbar^3} \sum_p \left[1 / \left(\omega_s - \Omega - J'_{k_s} + i \frac{\tilde{\Gamma}}{2} \right) \left(\omega_2 - \Omega - J'_{k_2} + i \frac{\tilde{\Gamma}}{2} \right) \left(\omega_1 - \Omega - J'_{k_1} + i \frac{\tilde{\Gamma}}{2} \right) \left(\omega_3 - \Omega - J'_{k_3} + i \frac{\tilde{\Gamma}}{2} \right) \right] \\ &\times \left\{ \left(\omega_1 - \Omega - J'_{k_1} + i \frac{\tilde{\Gamma}}{2} \right) \phi_M(k_1 - k_2) - i\Gamma \phi_M(k_1 - k_2) \left[\frac{J'_{k_3}}{(\omega_2 - \omega_1 - i\tilde{\Gamma}) I_M(k_1 - k_2)} \right. \right. \\ &\left. \left. + (J'_{k_2} - J'_{k_1}) \psi_M(k_1, k_2) \right] + \frac{1}{2} \frac{(J'_{k_1} + J'_{k_3})}{[1 - \Gamma_0 \kappa_M(k_3 + k_1)]} \right\} S(\omega_s, k_s) S(\omega_1, k_1) S(\omega_2, k_2) S(\omega_3, k_3), \end{aligned} \quad (5.10)$$

where

$$\phi_M(k_1 - k_2) \equiv 1 / \left[1 + \frac{i\Gamma}{(\omega_2 - \omega_1 - i\tilde{\Gamma}) I_M(k_1, k_2)} \right], \quad (5.11)$$

$$I_M(k_1, k_2) \equiv \left[\frac{1}{M} \sum_q \frac{1}{(\omega_2 - \omega_1 - J'_{k_2+q} + J'_{k_1+q} - i\tilde{\Gamma})} \right] \times (\omega_2 - \omega_1 - i\tilde{\Gamma}),$$

$$q = \frac{2\pi}{M} p, \quad p = 0, 1, 2, \dots, M-1. \quad (5.12)$$

$$\Psi_M(k_1, k_2) \equiv \frac{1}{2} \frac{[1 - I_M^{-1}(k_1, k_2)]}{J'_{k_2} - J'_{k_1}}, \quad (5.13)$$

$$\begin{aligned} \kappa_M(k_3 + k_1) &\equiv \frac{1}{M} \sum_q \frac{\cos^2(q)}{(\omega_3 + \omega_1 - 2\Omega - J'_{k_3+k_1-q} - J'_q + i\tilde{\Gamma})}, \end{aligned} \quad (5.14)$$

$$S(\omega_j, k_j) \equiv \frac{\omega_j - \Omega - J'_{k_j} + i(\tilde{\Gamma}/2)}{\omega_j - \Omega - J_{k_j} + i(\tilde{\Gamma}/2)}. \quad (5.15)$$

The auxiliary function introduced in Sec. IV (ϕ, I, ψ , and κ) can be obtained from ϕ_M, I_M, ψ_M , and κ_M by specializing to nearest-neighbor interactions and sending $M \rightarrow \infty$. For $M = 1$ we recover the familiar local-field approximation and the four $S(\omega_j, k_j)$ factors represent the local field corrections.^{1,2} In a three-dimensional system, $S(\omega_j, k_j)$ may be expressed in terms of the dielectric function $\epsilon(k_j, \omega_j) \equiv 1 + 4\pi\chi^{(1)}(k_j, \omega_j)$, and is given by $[\epsilon(k_j, \omega_j) + 2]/3$. For $M \rightarrow \infty$ and using a nearest-neighbor coupling J_k we recover the result of the previous section [Eq. (4.18)]. Of course, we expect that for large systems $N_c \ll N$. Equation (5.10) could then hold when $N_c < M \ll N$. This is the regime when the present form of the equations [Eqs. (5.4)–(5.6) together with Eq. (5.10)] should be most useful.

VI. CALCULATIONS AND DISCUSSION

We shall now present numerical calculations of $\chi^{(3)}$ which will illustrate the relative role of the three types of nonlinearities. In all the calculations presented below we have used the nearest-neighbor interaction ($J_k = 2V \cos k$) and neglected any explicit dependence on light wave vectors (the long wavelength approximation) setting $k_1 = k_2$

$= k_3 = 0$. By monitoring the convergence of Eq. (5.10) as M is increased, we establish the existence of the nonlinear coherence-size N_c , and analyze the factors affecting it. We shall focus our analysis on two four wave mixing techniques: two-photon absorption, and third harmonic generation. The two-photon absorption signal is given by

$$W_{\text{TPA}} = \text{Im} \chi_{\text{TPA}}^{(3)}, \quad (6.1)$$

where

$$\chi_{\text{TPA}}^{(3)} \equiv \chi^{(3)}(-k - \omega; k\omega, -k - \omega, k\omega). \quad (6.2)$$

Positive values of W_{TPA} correspond to two-photon absorption whereas negative values represent a bleaching (saturated absorption). The third harmonic signal is given by

$$W_{\text{THG}} = |\chi_{\text{THG}}^{(3)}|^2, \quad (6.3)$$

where

$$\chi_{\text{THG}}^{(3)} \equiv \chi^{(3)}(-3k - 3\omega; k\omega, k\omega, k\omega), \quad (6.4)$$

$\chi_{\text{THG}}^{(3)}$ is obtained from Eq. (4.18) by simply changing the sign of k_2 and ω_2 .

In Fig. 1 we display the real part, the imaginary part, and the absolute magnitude of $\chi^{(1)}, \chi_{\text{TPA}}^{(3)}$, and $\chi_{\text{THG}}^{(3)}$. The calculations were made using Eq. (4.18). $\chi_{\text{THG}}^{(3)}$ is shown in the vicinity of the single photon resonance $\omega \sim \Omega_0$ and the three photon resonance $\omega \sim \Omega_0/3$, where $\Omega_0 \equiv \Omega - 2|V|$ is the band edge frequency. In Fig. 2 we show the contributions of the cubic nonlinearity (CN), exciton population (EP), and two-exciton (TE) terms to the TPA, and to the THG signals. The dependence of the four wave mixing signals on the three phonon-induced relaxation parameters (Γ, Γ'_0 , and Γ''_0) is shown in Fig. 3 (for W_{TPA}) and in Fig. 4 (for W_{THG}). The THG signal in the vicinity of $\omega \sim \Omega_0/3$ does not vary with Γ_0 , we therefore only display its variation with Γ .

All the above calculations were based on the general expression for $\chi^{(3)}$ [Eq. (4.18)]. In the following we use the expression derived in Sec. V [Eq. (5.10)] which provides an operational definition of the nonlinear coherence-size N_c which controls the magnitude of the optical nonlinearity. We first consider the variation of the local-field switching function $C(M) \equiv J''_{k=0}/J_{k=0}$ [Eqs. (5.7) and (5.9)] with M . For $M = 1$ all intermolecular interactions are incorporated via the local-field and $C = 1$. As M increases, the local-field corrections become smaller and $C(M) \rightarrow 0$. This behavior is illustrated in Fig. 5.

The most dramatic effect of taking a finite M value is the appearance of TE and biexciton resonances in $\chi^{(3)}$. These resonances come from the TE contribution to $\chi^{(3)}$ [the third

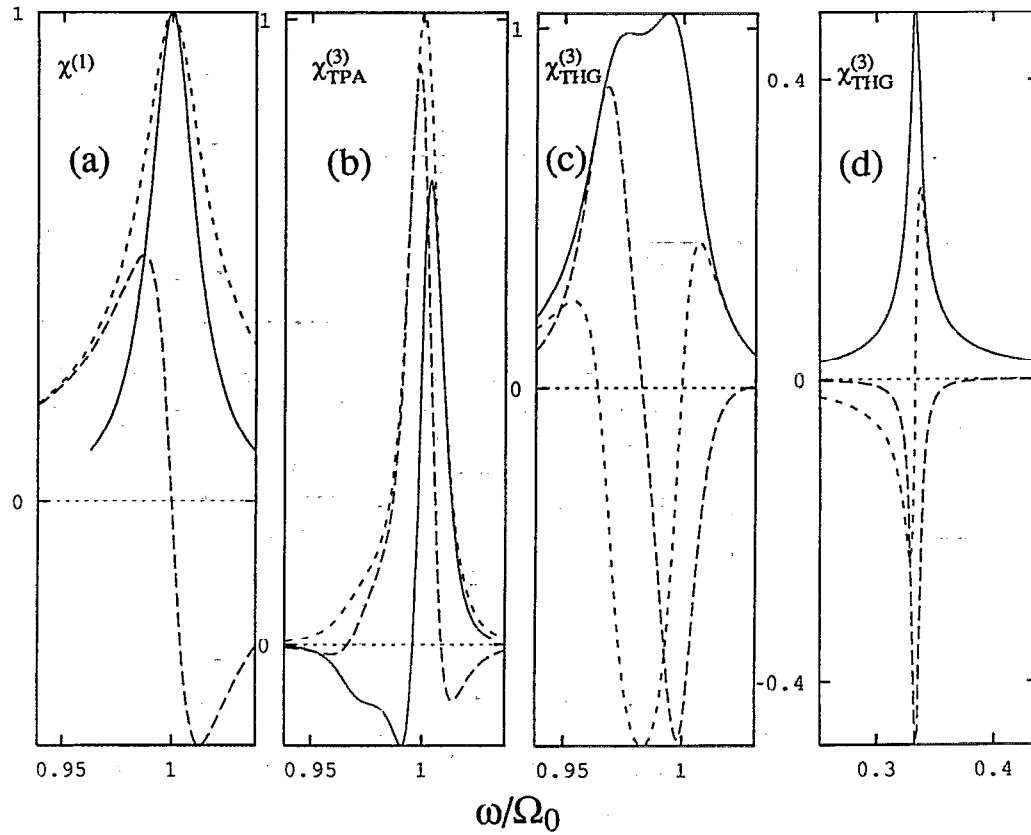


FIG. 1. Frequency dependence of the linear and nonlinear susceptibilities. Solid line: $\text{Im } \chi$; long dash: $\text{Re } \chi$; short dash: $|\chi|$. Phonon relaxation parameters are given in units of $|V| = 1$. $\Gamma = \gamma = 0.1$; $\Gamma_0' = -3$; $\Gamma_0'' = -0.01$; $V = -1$; $\Omega = 10$. (a) $\chi^{(1)}(\omega)$; (b) $\chi_{\text{TPA}}^{(3)}$; (c) $\chi_{\text{THG}}^{(3)}$ in the vicinity of the band edge; (d) $\chi_{\text{THG}}^{(3)}$ in the vicinity of the three photon resonance $\omega \sim \Omega_0/3$.

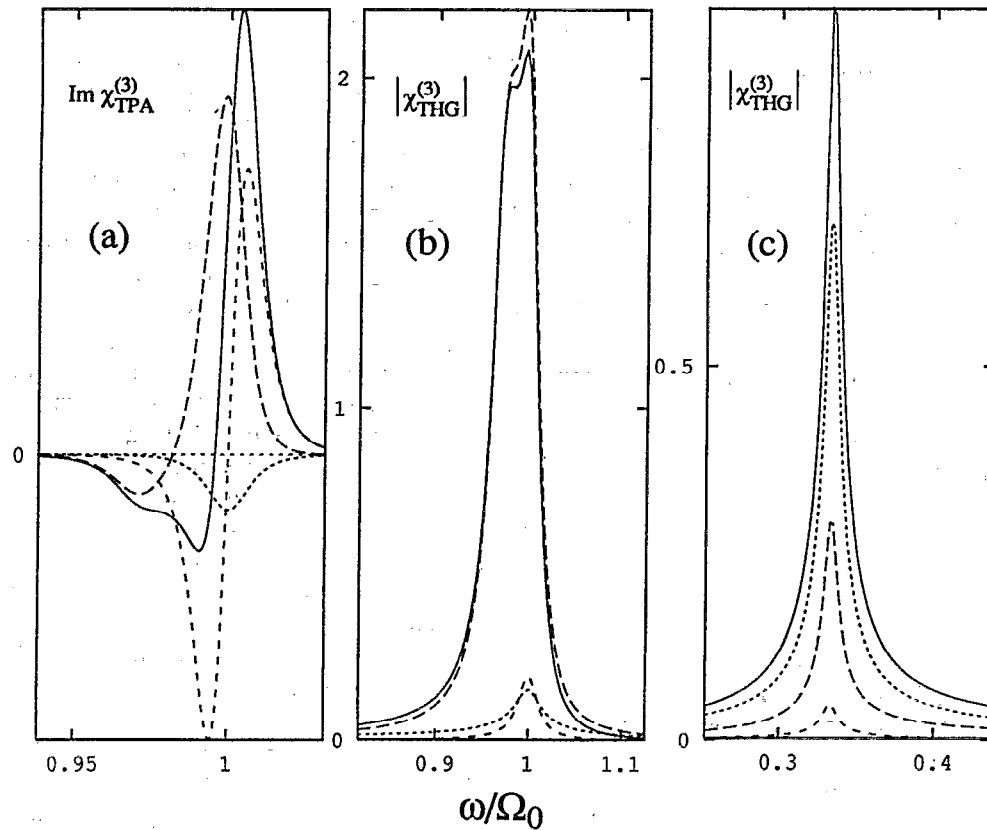


FIG. 2. The contribution of the CN, EP, and TE terms to $\chi^{(3)}$ representing TPA and THG. $\Gamma = \gamma = 0.1$; $\Gamma_0' = -3$; $\Gamma_0'' = -0.01$; $V = -1$. Solid line: total $\chi^{(3)}$; long dash: TE contribution; medium dash: EP contribution; short dash: CN contribution. (a) TPA signal \mathcal{W}_{TPA} ; (b) $|\chi_{\text{THG}}^{(3)}|$, square root of the THG signal in the vicinity of the band edge; (c) same as (b) in the vicinity of the three-photon resonances $\omega \sim \Omega_0/3$.

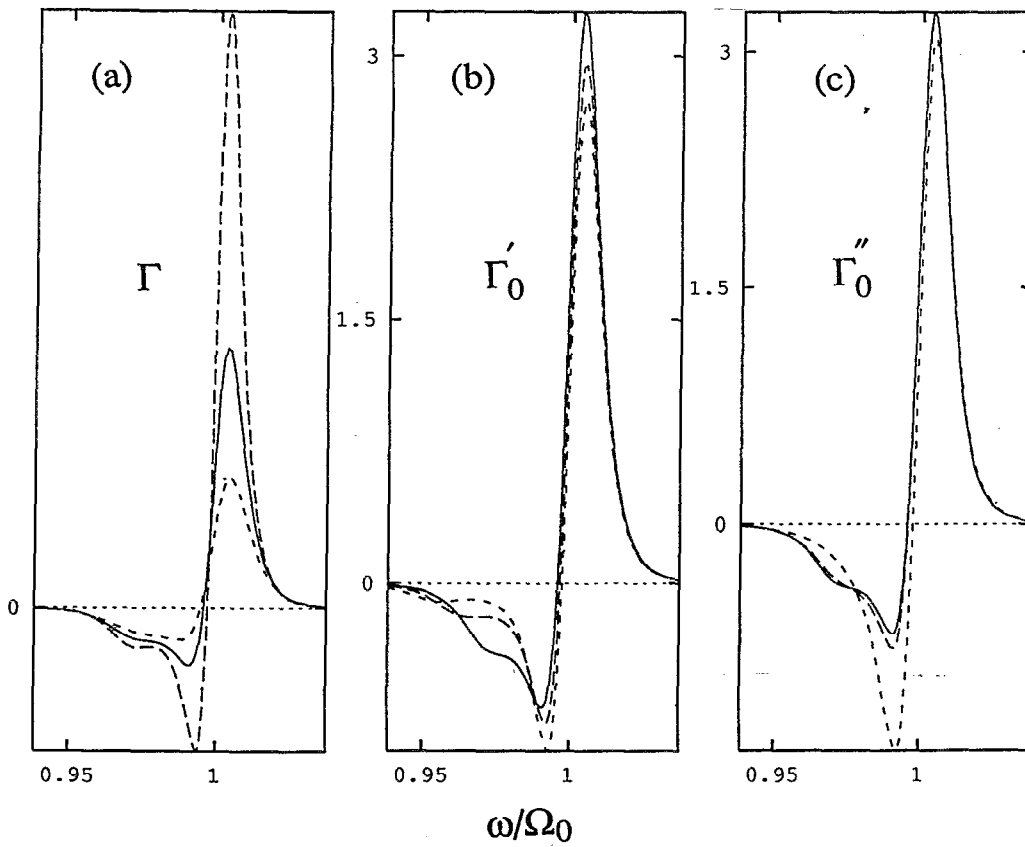


FIG. 3. Dependence of the TPA signal W_{TPA} on the phonon relaxation parameters (all given in units of $|V|=1$). (a) Solid: $\Gamma = \gamma = 0.1$; long dash: $\Gamma = \gamma = 0.08$; short dash: $\Gamma = \gamma = 0.12$. $\Gamma'_0 = -3$; $\Gamma''_0 = -0.01$; $V = -1$. (b) Solid: $\Gamma'_0 = -3$; long dash: $\Gamma'_0 = -3.5$; short dash: $\Gamma'_0 = -4$. $\Gamma = \gamma = 0.1$; $\Gamma''_0 = -0.01$; $V = -1$. (c) Solid: $\Gamma''_0 = -0.01$; long dash: $\Gamma''_0 = -0.1$; short dash: $\Gamma''_0 = -1$. $\Gamma = \gamma = 0.1$; $\Gamma'_0 = -3$; $V = -1$.

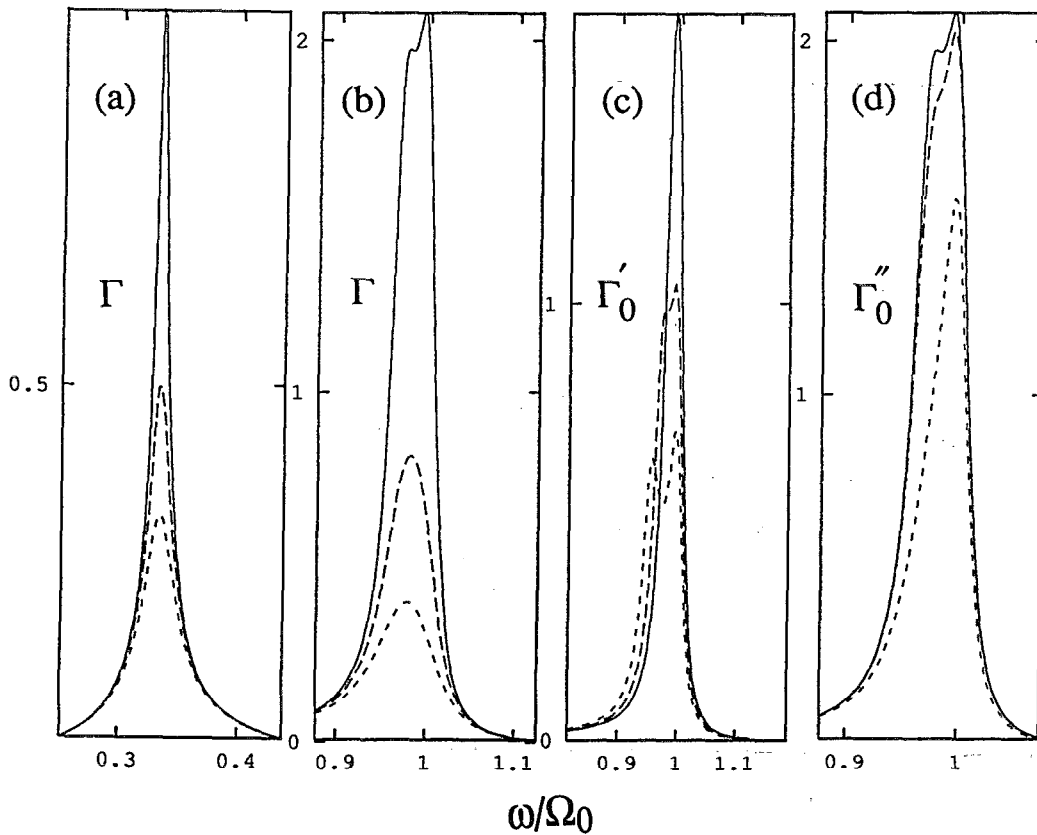


FIG. 4. Dependence of the square root of the THG signal $W_{\text{THG}}^{1/2}$ on the phonon relaxation parameters (all given in units of $|V|=1$). (a) Variation with Γ in the vicinity of the three photon resonance. solid: $\Gamma = \gamma = 0.1$; long dash: $\Gamma = \gamma = 0.2$; short dash: $\Gamma = \gamma = 0.3$. $\Gamma'_0 = -3$; $\Gamma''_0 = -0.01$; $V = -1$. (b) Variation with Γ in the vicinity of the band edge. Solid line: $\Gamma = \gamma = 0.1$; long dash: $\Gamma = \gamma = 0.2$; short dash: $\Gamma = \gamma = 0.3$. $\Gamma'_0 = -3$; $\Gamma''_0 = -0.01$; $V = -1$. (c) Variation with Γ'_0 in the vicinity of the band edge. Solid: $\Gamma'_0 = -2$; long dash: $\Gamma'_0 = -3$; short dash: $\Gamma'_0 = -4$. $\Gamma = \gamma = 0.1$; $\Gamma''_0 = -0.01$; $V = -1$. (d) Variation with Γ''_0 in the vicinity of the edge. solid: $\Gamma''_0 = -0.01$; long dash: $\Gamma''_0 = -0.1$; short dash: $\Gamma''_0 = -1$. $\Gamma = \gamma = 0.1$; $\Gamma'_0 = -3$; $V = -1$.

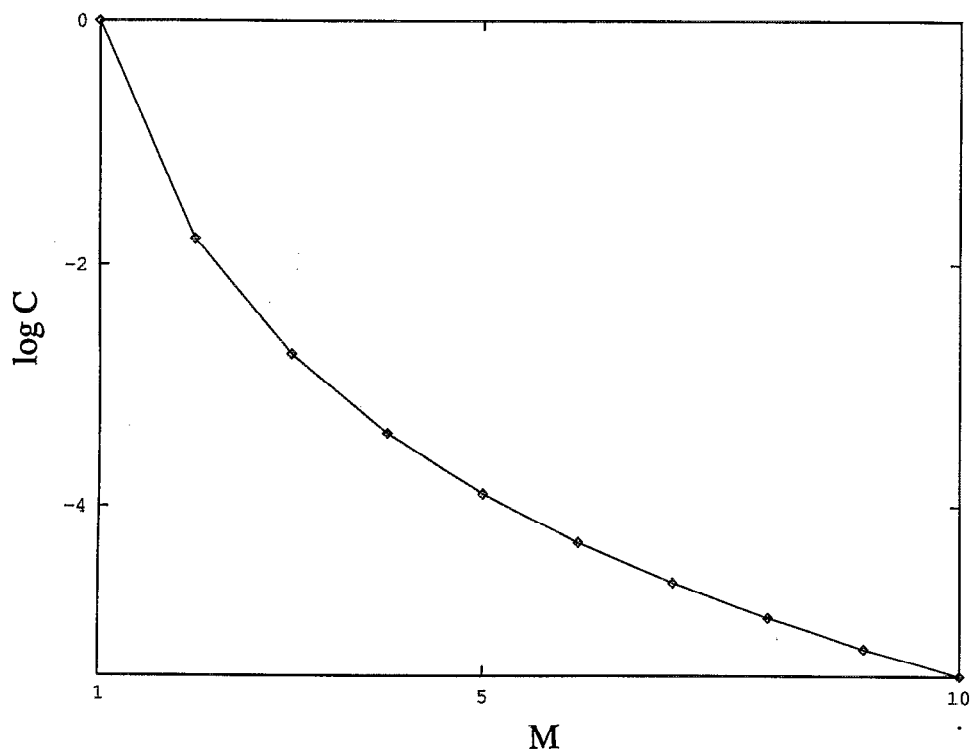


FIG. 5. The local-field switching function $C \equiv J''_{k=0}/J_{k=0}$. For $M=1$, $C=1$, and the local-field correction is the largest. As M increases, $C \rightarrow 0$ and the local-field correction becomes smaller.

term in the curly brackets in Eq. (5.10)], and occur when the denominator $1 - \Gamma_0 \kappa_M$ vanishes. Using Eq. (5.12) this results in the following equation:

$$1/\Gamma_0 = \frac{1}{M} \sum_q \frac{\cos^2 q}{(\omega_1 + \omega_3 - 2\Omega - 4V \cos q + i\tilde{\Gamma})}. \quad (6.5)$$

The TE resonances occur whenever $\omega_1 + \omega_3$ satisfy Eq. (6.5). In Fig. 6 we display the TPA signal calculated using Eq. (5.10) with $M=100$, for various values of the phonon mediated attractive interaction Γ'_0 . All curves show a progression of two-photon resonances in the TE band. These resonances are blue-shifted compared with the band edge ($\omega > \Omega_0$). The blue shift results from the Pauli exclusion

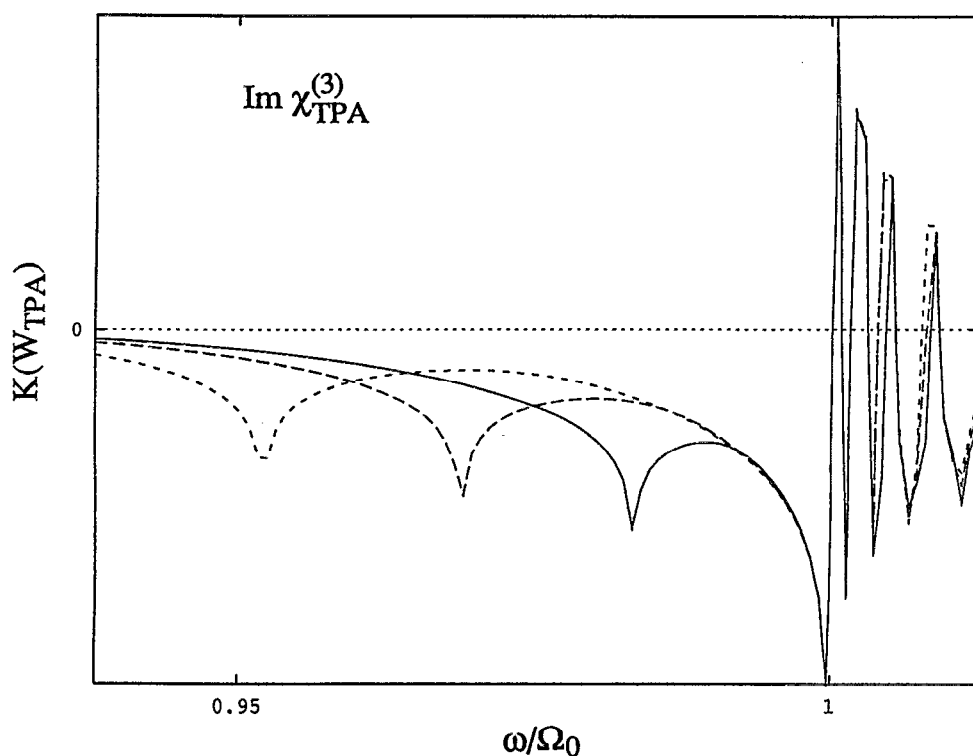


FIG. 6. Dependence of the TPA signal on the phonon-induced attraction Γ'_0 . Shown is the function $K(W_{\text{TPA}})$ [see Eq. (6.6)]. Calculations were made using Eq. (5.10) with $M=100$; $\Gamma = \gamma = 0.001$; $\Gamma''_0 = 0.0$. Solid line: $\Gamma'_0 = -2$; long dash: $\Gamma'_0 = -3$; short dash: $\Gamma'_0 = -4$.

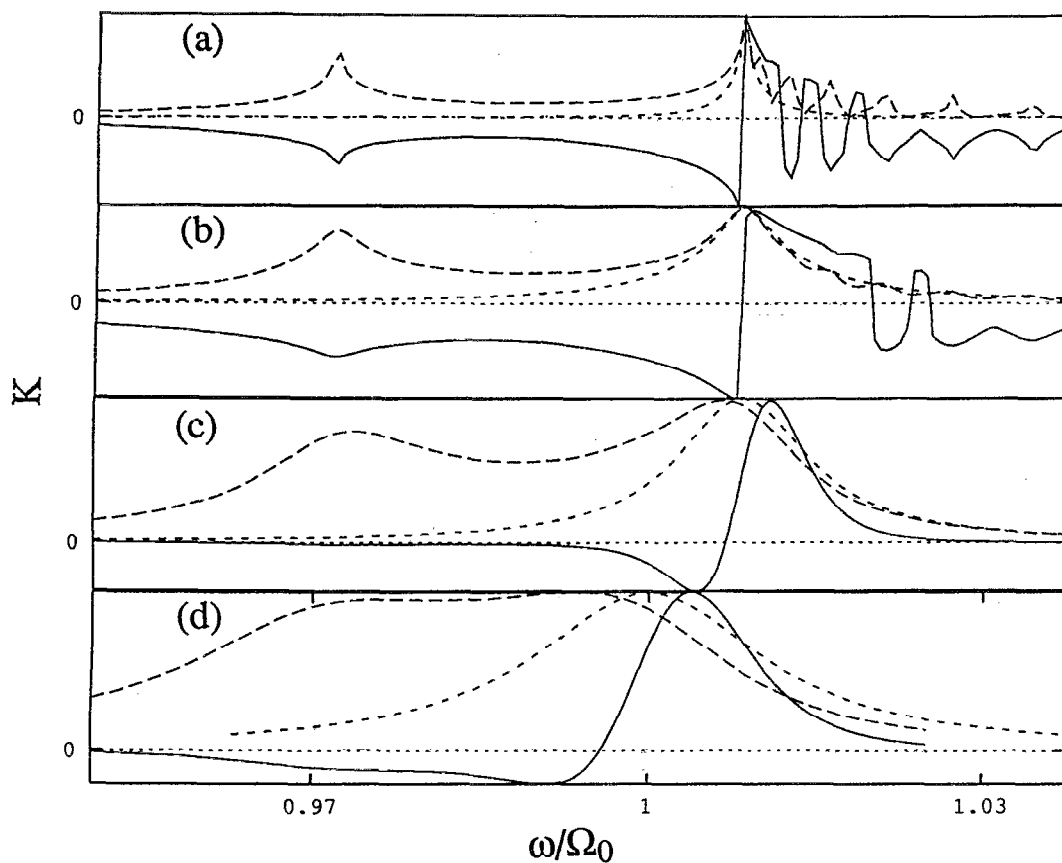


FIG. 7. Frequency dependence of the linear and nonlinear susceptibilities [Eq. (5.10)]. Shown is the function $K(x)$ [see Eq. (6.6)]. Solid line: $x = \text{Im } \chi_{\text{TPA}}^{(3)}$; long dash: $x = |\chi_{\text{TPA}}^{(3)}|$; $\Gamma_0' = -3.0$, $\Gamma_0'' = 0$, $M = 100$; short dash: $x = \text{Im } \chi^{(1)}(\omega)$. (a) $\Gamma = \gamma = 0.001$; (b) $\Gamma = \gamma = 0.01$; (c) $\Gamma = \gamma = 0.05$; (d) $\Gamma = \gamma = 0.1$.

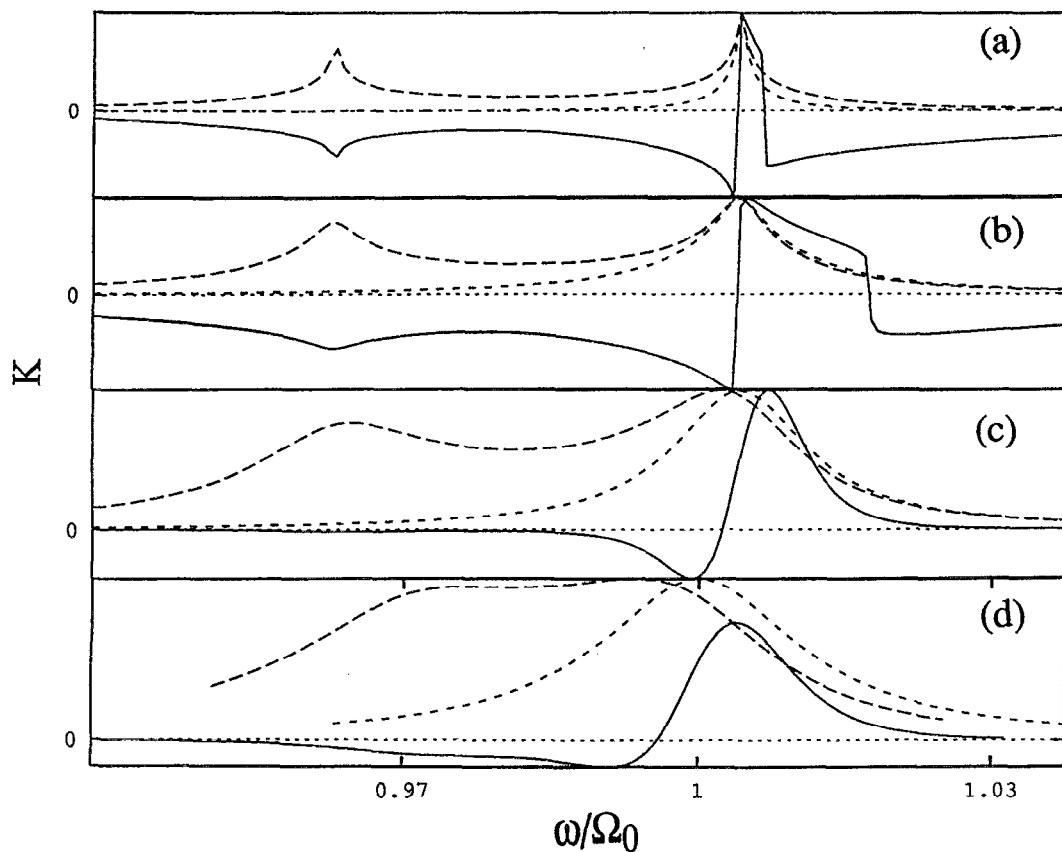


FIG. 8. Frequency dependence of the linear and nonlinear susceptibilities Eqs. (3.7) and (4.18). Shown is the function $K(x)$ [see Eq. (6.6)]. Solid line: $x = \text{Im } \chi_{\text{TPA}}^{(3)}$; $\Gamma_0' = -3.0$, $\Gamma_0'' = 0$; long dash: $x = |\chi_{\text{TPA}}^{(3)}|$; short dash: $x = \text{Im } \chi^{(1)}(\omega)$. (a) $\Gamma = \gamma = 0.001$; (b) $\Gamma = \gamma = 0.01$; (c) $\Gamma = \gamma = 0.05$; (d) $\Gamma = \gamma = 0.1$.

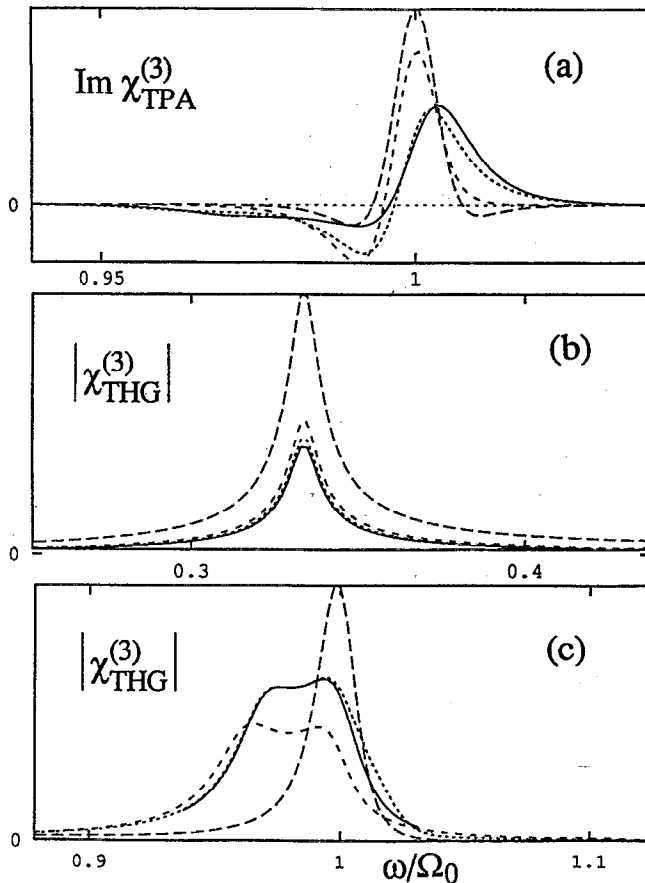


FIG. 9. Dependence of the nonlinear susceptibilities on the truncation size M , for an infinite chain $N \rightarrow \infty$ demonstrating the coherence-size. (a) TPA signal $\text{Im } \chi_{\text{TPA}}^{(3)}$. Solid: $M = N$; long dash: $M = 1$; medium dash: $M = 3$; short dash: $M = 6$. (b) Square root of the THG signal $|\chi_{\text{THG}}^{(3)}|$ in the vicinity of the three photon resonance. Solid line: $M = N$; long dash: $M = 1$; medium dash: $M = 2$; short dash: $M = 3$. (c) Same as (b) in the vicinity of the band edge. Solid line: $M = N$; long dash: $M = 1$; medium dash: $M = 6$; short dash: $M = 12$.

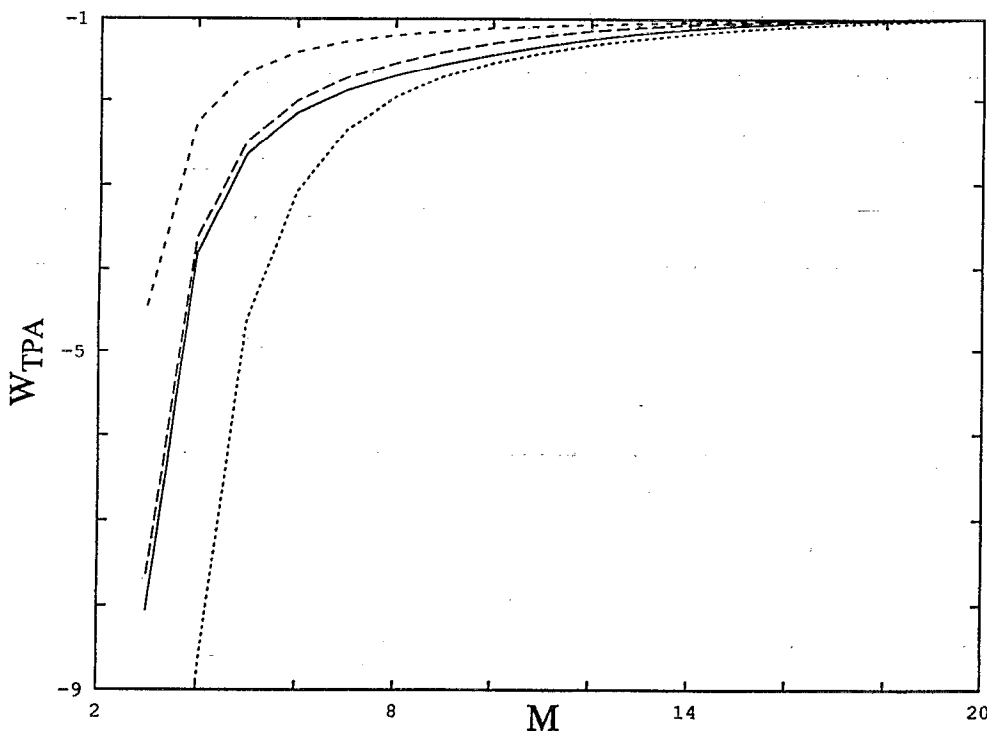


FIG. 10. Dependence of the TPA signal $[\text{Im } \chi_{\text{TPA}}^{(3)}]$ on the truncation size M , for various values of the phonon relaxation parameters. Solid line: $\Gamma = \gamma = 0.1$; $\Gamma_0' = -3$; $\Gamma_0'' = -0.01$; long dash: $\Gamma = \gamma = 0.1$; $\Gamma_0' = -4$; $\Gamma_0'' = -0.01$; middle dash: $\Gamma = \gamma = 0.1$; $\Gamma_0' = -3$; $\Gamma_0'' = -3.0$; short dash: $\Gamma = \gamma = 0.01$; $\Gamma_0' = -3$; $\Gamma_0'' = -0.01$.

which acts as an effective repulsion among excitons. In addition, we see an exciton bound resonance (biexciton) which is red-shifted ($\omega < \Omega_0$). The red shift increases with the binding energy Γ_0' , as is clearly shown in the figure. It should be noted that in the present model the exciton-exciton interaction has a repulsive and an attractive part. Both contributions have a different dependence on interexciton separation $|n - m|$. The Pauli repulsive part exists only for $n = m$ whereas the attractive part for $m = n \pm 1$. The Green function D requires solving the eigenvalue problem with both potentials present. We then find that when the attractive part is sufficiently strong, a new bound (biexciton) state will be found. The attractive phonon-mediated interaction is totally analogous to the attraction of two electrons in the theory of superconductivity (the Cooper pair).¹⁴ Since W_{TPA} may change sign, and we wish to display it on a log scale, we have plotted the following function:

$$K(x) \equiv \frac{x}{|x|} \log(1 + |x|), \quad (6.6)$$

where $x = W_{\text{TPA}}$, for $|x| \gg 1$, $K = (\text{sign } x) \log|x|$, whereas $K \sim x$ for $|x| \sim 0$. In Fig. 7(a) we compare the linear absorption, TPA, and THG signals for $M = 100$. Both TPA and THG show the TE and biexciton resonances discussed above [Eq. (6.5)]. The linear absorption does not show these resonances. As the phonon-induced damping is increased, these resonances broaden and gradually disappear. This is illustrated in Figs. (7b), (7c), and (7d). Figure 8 is completely analogous to Fig. 7, except that we do not invoke the local-field approximation, taking $M = N$ with $N \rightarrow \infty$ [Eq. (4.18)]. As was shown previously,¹² the TE resonances do not show up here, since as M increases they become very close and eventually merge and disappear. The reason is that the system becomes less anharmonic as M increases since the Pauli exclusion becomes less effective in this case.¹² The

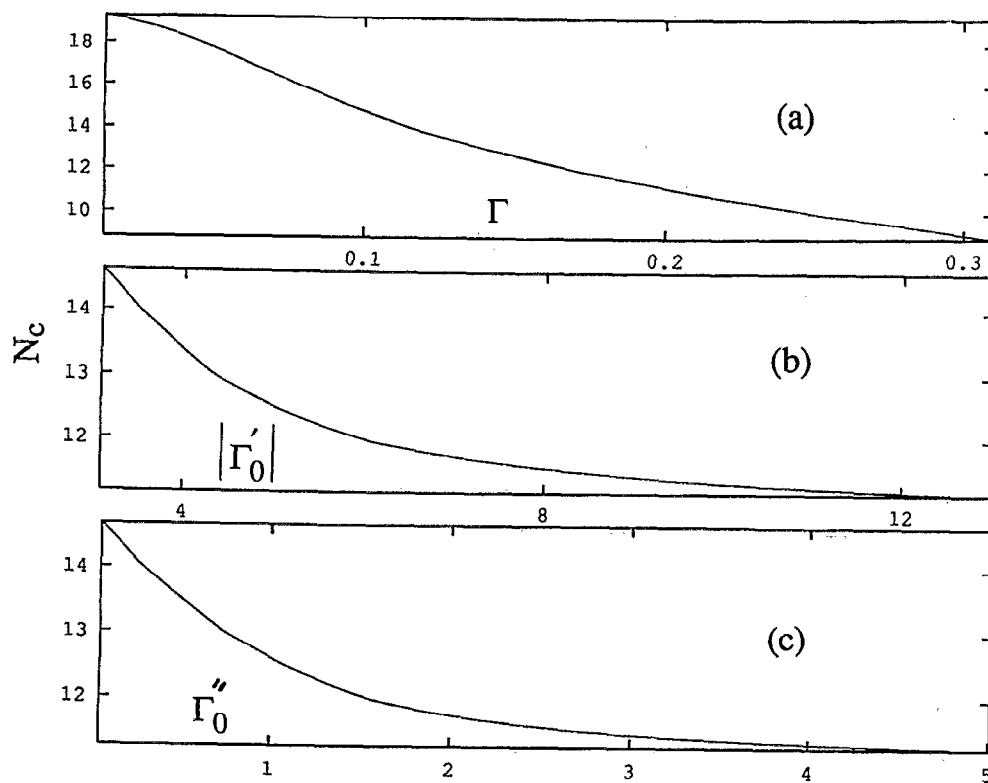


FIG. 11. The dependence of the coherence-size N_c , defined using TPA [Eq. (6.7)], on the phonon relaxation parameters. (a) Dependence on Γ . $\Gamma'_0 = -3$; $\Gamma''_0 = -0.01$; $\omega - \Omega_0 = -0.08$; $V = -1$. $\Gamma = \gamma$ is varied in the range 0.01–0.03. (b) Dependence on Γ'_0 . $\Gamma''_0 = -0.01$; $\omega - \Omega_0 = -0.08$; $V = -1$. Γ'_0 is varied in the range -12 to -3 . (c) Dependence on Γ''_0 . $\Gamma = \gamma = 0.1$; $\Gamma'_0 = -3$; $\omega - \Omega_0 = -0.08$; $V = -1$; Γ''_0 is varied in the range -5.00 to -0.01 .

biexciton resonance does show up for small damping rates [Fig. 8(a)], but gradually disappears as the damping is increased [Figs. (8b), (8c), and (8d)]. It should be noted that the phonon-mediated interaction Γ'_0 could be either attractive or repulsive. In the present calculations we have taken it to be attractive (Γ'_0 negative). For a repulsive interaction,

the biexciton resonance will appear above the TE band, and is more likely to be broadened by the decay channel provided by the TE states.

The convergence of $\chi^{(3)}$ with M is shown in Fig. 9. A clearer picture may be provided by looking at the TPA signal at a given frequency $\omega - \Omega = 0.08$ V and plotting it vs M .

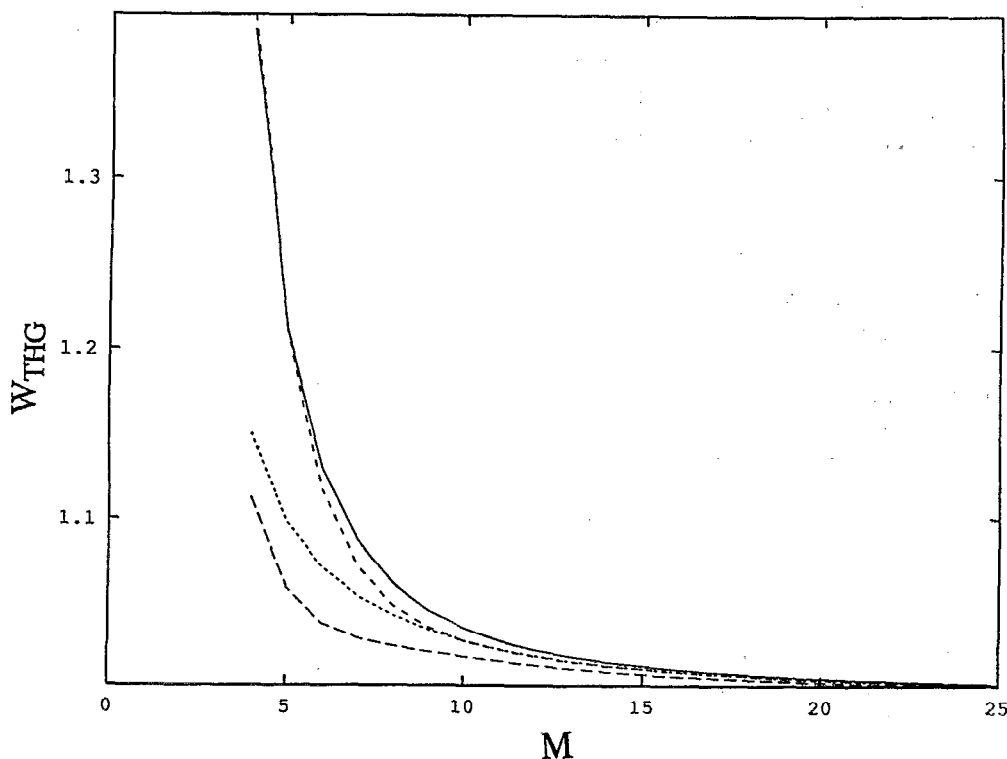


FIG. 12. Dependence of the THG signal W_{THG} on the truncation size M , for various values of the phonon relaxation parameters, for $\omega - \Omega_0 = -0.5$, $V = -1$. Solid line: $\Gamma = \gamma = 0.01$; $\Gamma'_0 = -3$, $\Gamma''_0 = -0.01$; long dash: $\Gamma = \gamma = 0.4$; $\Gamma'_0 = -3$; $\Gamma''_0 = -0.01$; middle dash: $\Gamma = \gamma = 0.01$; $\Gamma'_0 = -3.2$; $\Gamma''_0 = -0.01$; short dash: $\Gamma = \gamma = 0.01$; $\Gamma'_0 = -3$; $\Gamma''_0 = -2.0$.

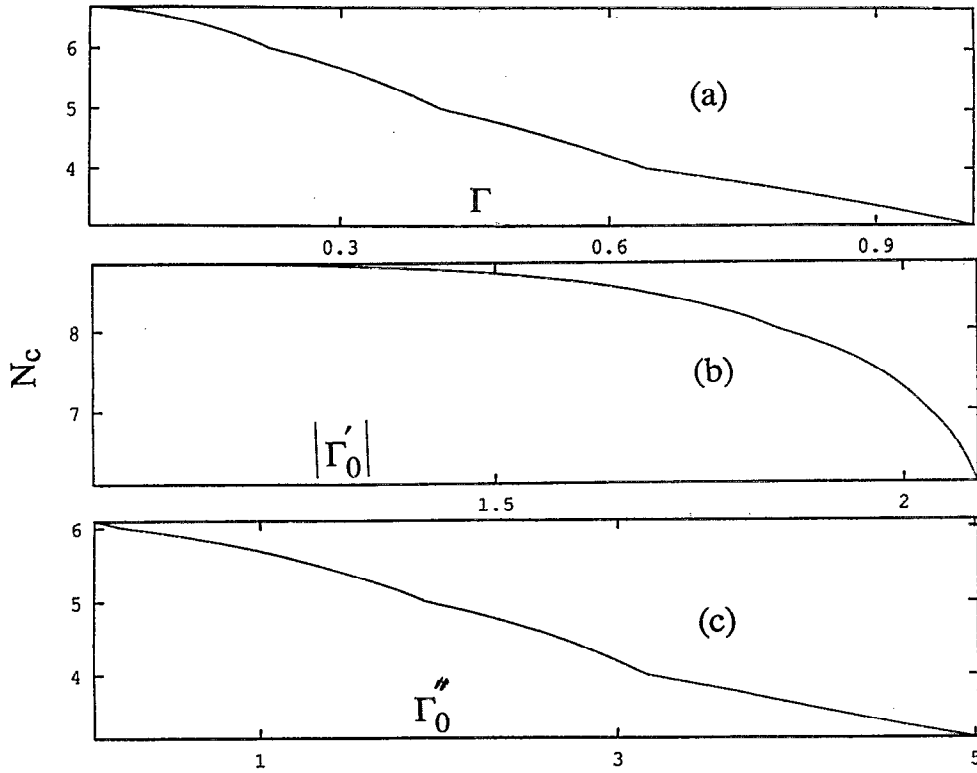


FIG. 13. The dependence of the coherence-size N_c defined using the THG [Eq. (6.8)] on the phonon relaxation parameters. (a) Dependence on Γ varied in the range 0.01–1. $\Gamma'_0 = -1$; $\Gamma''_0 = -0.01$; $\omega - \Omega_0 = -0.5$; $V = -1$; $\gamma = \Gamma$. (b) Dependence on Γ'_0 . $\Gamma = \gamma = 0.1$; $\Gamma''_0 = -0.04$; $\omega - \Omega_0 = -0.2$; $V = -1$. Γ'_0 is varied in the range -1.0 to -2.0 . (c) Dependence on Γ''_0 . $\Gamma'_0 = -1$; $\Gamma = \gamma = 0.2$; $\omega - \Omega_0 = -0.5$; $V = -1$. Γ''_0 is varied in the range -0.02 to -5.0 .

This is shown in Fig. 10 for different values of the damping. As expected, when the damping is increased, the coherence-size decreases and the saturation occurs for smaller values of M . Figure 10 allows us to introduce the following operational definition of the nonlinear coherence-size N_c :

$$|W_{\text{TPA}}(M = N_c) - W_{\text{TPA}}(M \rightarrow N)| = 0.1 |W_{\text{TPA}}(M \rightarrow N)|. \quad (6.7)$$

N_c is thus defined to be the value of M for which $\chi^{(3)}$ attains 90% of its asymptotic ($M = N$) value. N_c defined that way is displayed in Fig. 11 as a function of the various phonon-coupling parameters Γ , Γ'_0 , Γ''_0 . Figures 12 and 13 are analogous to Figs. 10 and 11, except that the calculation is made for THG. N_c is then similarly defined by

$$|W_{\text{THG}}(M = N_c) - W_{\text{THG}}(M \rightarrow N)| = 0.1 |W_{\text{THG}}(M \rightarrow N)|. \quad (6.8)$$

The values of N_c obtained from THG (Fig. 13) are very similar to those of Fig. 11. We believe that the concept of the nonlinear coherence size introduced in this article is very general, and should have important implications on the interpretation of the nonlinear optical response in condensed phases (whether bulk or restricted geometries). An application to semiconductor nanostructures²⁶ is also a natural extension of the present results.

ACKNOWLEDGMENTS

The support of the Center for Photoinduced Charge Transfer sponsored by the National Science Foundation, and the Air Force Office of Scientific Research, is gratefully acknowledged.

APPENDIX A: THE NONLINEAR-OSCILLATOR EQUATIONS OF MOTION

The equations of motion will be derived by starting with the Heisenberg equation for an arbitrary operator A ,

$$\frac{1}{i} \frac{d}{dt} A = [H, A]. \quad (\text{A1})$$

Taking $A = B_k$, $B_{k_1}^\dagger B_{k_2}$, $B_{k_1} B_{k_2}$, and b_q which represent polarization (P), exciton population (EP), two-exciton (TE), and phonon variables, respectively, and using the Hamiltonian Eq. (2.1) we get

$$\begin{aligned} \frac{1}{i} \frac{d}{dt} B_k &= -\Omega B_k - J_k (B_k + B_{-k}^\dagger) - \sum_q F_{k,-q} B_{k-q} \\ &\times (b_q + b_{-q}^\dagger) + \frac{2}{N} \sum_{k',k''} J_{k'} B_{k'+k}^\dagger B_{k+k''} \\ &\times (B_{k'} + B_{-k'}^\dagger) - \frac{2(\mu\rho/\hbar)}{N\sqrt{N}} \sum_{k'} E(\vec{k}', t) \\ &\times \left[\sum_{k''} B_{k'+k''}^\dagger B_{k+k''} - \frac{N}{2} \delta_{k',k} \right], \end{aligned} \quad (\text{A2})$$

$$\begin{aligned} \frac{1}{i} \frac{d}{dt} B_{k_2}^\dagger B_{k_1} &= (J_{k_2} - J_{k_1}) B_{k_2}^\dagger B_{k_1} + \frac{1}{\sqrt{N}} (\mu\rho/\hbar) [B_{k_2}^\dagger E(k_1, t) \\ &- B_{k_1} E(k_2, t)] + \sum_q (F_{k_2,q} B_{k_2+q}^\dagger B_{k_1} \\ &- F_{k_1-q,q} B_{k_2}^\dagger B_{k_1-q}) (b_q + b_{-q}^\dagger), \end{aligned} \quad (\text{A3})$$

$$\begin{aligned} \frac{1}{i} \frac{d}{dt} B_{k_1} B_{k_3} = & - (2\Omega + J_{k_1} + J_{k_3}) B_{k_1} B_{k_3} \\ & + \mu\rho / (\hbar\sqrt{N}) [B_{k_1} E(k_3, t) + B_{k_3} E(k_1, t)] \\ & - \sum_q (F_{k_3-q, q} B_{k_1} B_{k_3-q} \\ & + F_{k_1-q, q} B_{k_1-q} B_{k_3}) (b_q + b_{-q}^\dagger) \end{aligned} \quad (A4)$$

$$\frac{1}{i} \frac{d}{dt} b_q = -\omega_q b_q - \frac{1}{\sqrt{N}} \sum_k F_{k, -q} B_{k-q}^\dagger B_k. \quad (A5)$$

The next step is to eliminate the phonon variables. In Ref. 11 this was done in detail for the *P* and EP equations. For the TE variables this can be done in a similar way, and will not be repeated here. When this is done, we finally obtain Eqs. (2.10) and (2.11).

APPENDIX B: TRUNCATION OF THE HIERARCHY: DERIVATION OF EQ. (2.12)

In this appendix we show how the hierarchy of equations is truncated, resulting in a closed set. We first neglect terms which are products of four *B* factors. These terms do not contribute to $\chi^{(3)}$ since they are fourth order in the field. The remaining problem is then to factorize the triple product of *B* factors. This is done by introducing the following ansatz for the density matrix at time *t*:

$$\begin{aligned} \rho(t) = s \exp \left[\sum_n (\beta_n B_n^\dagger + \beta_n^* B_n) \right. \\ \left. + \sum_{nm} (\gamma_{nm} B_n^\dagger B_n^\dagger + \gamma_{nm}^* B_n B_m + \kappa_{nm} B_n^\dagger B_m) \right]. \end{aligned} \quad (B1)$$

All the coefficients *s*, β , γ , and κ are time dependent. We can relate these coefficients to the expectation values of our relevant set of operators by expanding the exponential perturbatively. We thus have

$$\langle A \rangle = \text{Tr}[A\rho], \quad (B2)$$

$$\frac{1}{N} \sum_{q'} G_{k_2 k_1}(q + q') = \frac{1}{N\mu^2} \chi^{*(1)}(k_2 \omega_2) \chi^{(1)}(k_1 \omega_1) \left/ \left\{ 1 + i \frac{\Gamma}{N} \sum_q \frac{1}{[\omega_2 - \omega_1 - J_{k_2+q} + J_{k_1+q} - i(\Gamma + \gamma)]} \right\} \right. \quad (C2)$$

Upon the substitution of Eq. (C2) in Eq. (C1) we finally get

$$\begin{aligned} G_{k_2 k_1}(q) = & \frac{1}{\mu^2} \chi^{*(1)}(k_2 \omega_2) \chi^{(1)}(k_1 \omega_1) - i \frac{(\Gamma/N\mu^2)}{[\omega_2 - \omega_1 - J_{k_2+q} + J_{k_1+q} - i(\Gamma + \gamma)]} \\ & \times \frac{\chi^{*(1)}(k_2 \omega_2) \chi^{(1)}(k_1 \omega_1)}{\left\{ 1 + i \frac{\Gamma}{N} \sum_{q'} \frac{1}{[\omega_2 - \omega_1 - J_{k_2+q'} + J_{k_1+q'} - i(\Gamma + \gamma)]} \right\}}. \end{aligned} \quad (C3)$$

Adopting a nearest-neighbor approximation for the interaction *V* we get

$$J_k = 2V \cos k; \quad (C4)$$

and using Eqs. (C3) and (C4) we get

$$\begin{aligned} I_N(k_1, k_2) / (\omega_2 - \omega_1 - i\tilde{\Gamma}) \equiv & \frac{1}{N} \sum_q \frac{1}{\omega_2 - \omega_1 - J_{k_2+q} + J_{k_1+q} - i(\Gamma + \gamma)} \\ = & \frac{1}{N} \sum_q \frac{1}{\left[\omega_2 - \omega_1 - i\tilde{\Gamma} - 4V \sin\left(q + \frac{k_2 + k_1}{2}\right) \sin\left(\frac{k_1 - k_2}{2}\right) \right]}, \end{aligned} \quad (C5)$$

$$\langle 0|\rho|0 \rangle = s \left(1 + \frac{1}{2} \sum_n |\beta_n|^2 \right), \quad (B3)$$

$$\begin{aligned} \langle B_n \rangle = & s \left[\beta_n^* \left(1 + \frac{1}{2} \sum_m |\beta_m|^2 \right) \right. \\ & \left. + \frac{1}{2} \sum_m (\beta_m^* \kappa_{mn} + 2\beta_m \gamma_{mn}^*) \right], \end{aligned} \quad (B4)$$

$$\langle B_n^\dagger B_m \rangle = s \left(\kappa_{nm} + \beta_m^* \beta_n + \frac{1}{2} \delta_{nm} \sum_p |\beta_p|^2 \right), \quad (B5)$$

$$\langle B_n B_m \rangle = s (\beta_n^* \beta_m + 2\gamma_{nm}), \quad (B6)$$

$$s = \left[1 + \left(\frac{N}{2} + 2 \right) \sum_p |\beta_p|^2 + (2N - 1) \sum_p \kappa_{pp} \right]^{-1}. \quad (B7)$$

At this point we can close the hierarchy using the relation

$$\langle B_{k_1}^\dagger B_{k_2} B_{k_3} \rangle = \text{Tr} [B_{k_1}^\dagger(0) B_{k_2}(0) B_{k_3}(0) \rho(t)], \quad (B8)$$

where we use the Schrödinger picture, i.e., the operators are taken at *t* = 0 and the time evolution is included in the density matrix. Upon the substitution of Eq. (B1) in Eq. (B8) we get

$$\langle B_n^\dagger B_m B_p \rangle = s (\beta_n \beta_m^* \beta_p^* + 2\beta_n \gamma_{pm} + \beta_p^* \kappa_{nm} + \beta_m^* \kappa_{np}). \quad (B9)$$

When Eqs. (B4)–(B7) are substituted in Eq. (B9) we finally obtain Eq. (2.12).

APPENDIX C: DERIVATION OF EQ. (4.18)

In this appendix we solve for the Green functions *G* and *D* and derive the expression for $\chi^{(3)}$. We start by calculating *G*. Upon the substitution of Eq. (4.4) in (3.11a) we get

$$\begin{aligned} [\omega_2 - \omega_1 - J_{k_1+q} + J_{k_2} - i(\Gamma + \gamma)] G_{k_2 k_1}(q) \\ + i \frac{\Gamma}{N} \sum_{q'} G_{k_2 k_1}(q + q') \\ = (\rho/\hbar) [\chi^{*(1)}(k_2 \omega_2) - \chi^{(1)}(k_1 \omega_1)] \delta_{q,0}. \end{aligned} \quad (C1)$$

Using Eq. (C1) we get

for $N \rightarrow \infty$ we perform the summation and get Eq. (4.21)

$$\sum_q J_{k_1+q} G_{k_2 k_1}(q) = \frac{1}{\mu^2} \chi^{*(1)}(k_2 \omega_2) \chi^{(1)}(k_1 \omega_1) \left[J_{k_1} - i \frac{\Gamma}{2} \left(1 - \frac{1}{I} \right) \left(1 + \frac{i\bar{\Gamma}}{(\omega_2 - \omega_1 - i\bar{\Gamma})I} \right)^{-1} \right]. \quad (C6)$$

We next solve the equation for D . Using Eq. (3.14) together with Eq. (4.12) we get

$$\begin{aligned} & [\omega_3 + \omega_1 - 2\Omega - J_{k_1+q} - J_{k_3-q} + i(\Gamma + \gamma)] D_{k_1 k_3}(q) - \frac{\Gamma_0 \phi(k_1 - k_3 + 2q)}{N} \\ & \times \sum_{q'} \phi\left(q' + q + \frac{k_1 - k_3}{2}\right) D_{k_1 k_3}(q + q') = -(\rho/\hbar) [\chi^{(1)}(k_3 \omega_3) + \chi^{(1)}(k_1 \omega_1)] \delta_{q,0}, \end{aligned} \quad (C7)$$

where

$$\phi(k) = \cos(k). \quad (C8)$$

Repeating the same procedure used for G we solve Eq. (C7) resulting in

$$\begin{aligned} & \frac{1}{N} \sum_p \phi\left(p - \frac{k_1 - k_3}{2}\right) D_{k_1 k_3}(p) \\ & = \frac{1}{N\mu^2} \phi\left(\frac{k_1 - k_3}{2}\right) \chi^{(1)}(k_3 \omega_3) \chi^{(1)}(k_1 \omega_1) \left/ \left[1 - \frac{\Gamma_0}{N} \sum_{p'} \frac{\phi[(k_1 + k_3)/2 - p'] \phi[p' - (k_1 + k_3)/2]}{[\omega_3 + \omega_1 - 2\Omega - J_{k_3+k_1-p'} - J_{-p'} + i(\Gamma + \gamma)]} \right] \right., \end{aligned} \quad (C9)$$

$$\begin{aligned} D_{k_1 k_3}(q) & = \frac{1}{\mu^2} \chi^{(1)}(k_3 \omega_3) \chi^{(1)}(k_1 \omega_1) \\ & + \Gamma_0 \phi\left(\frac{k_3 - k_1}{2}\right) \phi\left(\frac{k_1 - k_3}{2}\right) \chi^{(1)}(k_3 \omega_3) \chi^{(1)}(k_1 \omega_1) / N\mu^2 [\omega_3 + \omega_1 - 2\Omega - J_{k_1+q} - J_{k_3-q} + i(\Gamma + \gamma)] \\ & \times \left\{ 1 - \frac{\Gamma_0}{N} \sum_{p'} \frac{\phi[(k_1 + k_3)/2 - p'] \phi[p' - (k_1 + k_3)/2]}{[\omega_3 + \omega_1 - 2\Omega - J_{k_3+k_1-p'} - J_{-p'} + i(\Gamma + \gamma)]} \right\}. \end{aligned} \quad (C10)$$

Equation (3.16) requires the evaluation of a sum involving D . Using Eq. (C10) we get

$$\sum_q J_{k_1+q} D_{k_1 k_3}(q) = \frac{1}{\mu^2} \chi^{(1)}(k_3 \omega_3) \chi^{(1)}(k_1 \omega_1) \left[J_{k_3} + \frac{1}{2}(J_1 + J_3) \frac{\Gamma_0 \kappa_N(k_s + k_2)}{1 - \Gamma_0 \kappa_N(k_s + k_2)} \right], \quad (C11)$$

where

$$\kappa_N(k_s + k_2) \equiv \frac{1}{N} \sum_p \cos^2\left(p - \frac{k_s + k_2}{2}\right) \left[\omega_3 + \omega_1 - 2\Omega - 4V \cos\left(\frac{k_s + k_2}{2}\right) \cos\left(p - \frac{k_s + k_2}{2}\right) + i\bar{\Gamma} \right]^{-1}. \quad (C12)$$

Upon the substitution of Eqs. (C3), (C6), (C10), and (C11), in Eq. (3.16) we get

$$\begin{aligned} & \chi^{(3)}(-k_s - \omega_s; k_1 \omega_1, -k_2 \omega_2, k_3 \omega_3) \\ & = \frac{2V^2}{N^2 \mu^2} \sum_p \frac{\chi^{*(1)}(k_2 \omega_2) \chi^{(1)}(k_1 \omega_1) \chi^{(1)}(k_3 \omega_3)}{\left(-\omega_s + \Omega + J_{k_s} - i \frac{\bar{\Gamma}}{2}\right)} \left(J_{k_3} \left[1 + \frac{i\bar{\Gamma}}{(\omega_2 - \omega_1 - i\bar{\Gamma})I_N(k_1, k_2)} \right]^{-1} \right. \\ & + \left\{ J_{k_1} - i \frac{\Gamma}{2} \left[1 - \frac{1}{I_N(k_1, k_2)} \right] \left[1 + i \frac{\Gamma}{(\omega_2 - \omega_1 - \bar{\Gamma})I_N(k_1, k_2)} \right]^{-1} \right\} \\ & + \left. \left\{ J_{k_3} + \frac{1}{2}(J_{k_1} + J_{k_3}) \frac{\Gamma_0 \kappa_N(k_s + k_2)}{[1 - \Gamma_0 \kappa_N(k_s + k_2)]} \right\} - 2J_{k_3} - \frac{(\rho/\hbar)\mu^2}{\chi^{(1)}(k_1 \omega_1)} \left[1 + i \frac{\Gamma}{(\omega_2 - \omega_3 - i\bar{\Gamma})I_N(k_1, k_2)} \right] \right). \end{aligned} \quad (C13)$$

Equation (C13) is identical to Eq. (4.24).

- ¹N. Bloembergen, *Nonlinear Optics* (Benjamin, New York, 1965); D. Bedeaux and N. Bloembergen, *Physica* **69**, 67 (1973).
- ²C. Flytzanis, in *Quantum Electronics V.I.*, edited by H. Rabin and C. L. Tang (Academic, New York, 1975), p. 1; Y. R. Shen, *The Principles of Nonlinear Optics* (Wiley, New York, 1984).
- ³(a) S. Mukamel, Z. Deng, and J. Grad, *J. Opt. Soc. Am. B* **5**, 804 (1988); (b) J. Knoester and S. Mukamel, *Phys. Rev. A* **39**, 1899 (1989); *J. Opt. Soc. Am. B* **6**, 643 (1988).
- ⁴A. S. Davydov, in *Theory of Molecular Excitons* (Plenum, New York, 1971).
- ⁵(a) G. J. Small, in *Excited States*, edited by E. C. Lim (Academic, New York, 1982); (b) S. H. Stevenson, M. A. Connolly, and G. J. Small, *Chem. Phys.* **128**, 157 (1988).
- ⁶K. E. Schriver, M. Y. Hahn, and R. L. Whetten, *Phys. Rev. Lett.* **59**, 1066 (1987).
- ⁷E. Hanamura, *Phys. Rev. B* **37**, 1273 (1988).
- ⁸F. C. Spano and S. Mukamel, *Phys. Rev. A* **40**, 7065 (1989).
- ⁹H. Ishihara and K. Cho, *Phys. Rev. B* **42**, 1724 (1990); *Nonlin. Opt.* **1** (in press, 1991).
- ¹⁰F. C. Spano, V. Agranovich, and S. Mukamel, *J. Chem. Phys.* **95**, 1400 (1991).
- ¹¹J. Knoester and S. Mukamel, *Phys. Rep.* **205**, 1 (1991).
- ¹²F. C. Spano and S. Mukamel, *Phys. Rev. Lett.* **66**, 1197 (1991); *J. Chem. Phys.* **95**, 7526 (1991).
- ¹³F. C. Spano, J. R. Kuklinski, and S. Mukamel, *Phys. Rev. Lett.* **65**, 211 (1990).
- ¹⁴G. D. Mahan, *Many Particle Physics* (Plenum, New York, 1990).
- ¹⁵D. S. Chemla and J. Zyss, *Nonlinear Optical Properties of Organic Molecules and Crystals* (Academic, New York, 1987), Vols. I and II.
- ¹⁶B. I. Greene, J. Orenstein, R. R. Millard, and L. R. Williams, *Phys. Rev. Lett.* **58**, 2750 (1987); B. I. Greene, J. Orenstein, and S. Schmitt-Rink, *Science* **247**, 679 (1990).
- ¹⁷P. D. Townsend, W.-S. Fann, S. Etemad, G. L. Baker, Z. G. Soos, and P. C. M. McWilliams, *Chem. Phys. Lett.* **180**, 485 (1991); Z. G. Soos and G. W. Hayden, *Chem. Phys.* **143**, 199 (1990); S. Etemad and Z. G. Soos, in *Spectroscopy of Advanced Materials*, edited by R. J. H. Clark and R. E. Hester (Wiley, New York, 1991), p. 87.
- ¹⁸G. J. Blanchard and J. P. Heritage, *Chem. Phys. Lett.* **177**, 287 (1991); W.-S. Fann, S. Benson, J. M. J. Madey, S. Etemad, G. L. Baker, and F. Kajzar, *Phys. Rev. Lett.* **62**, 1492 (1989).
- ¹⁹J. R. G. Thorne, Y. Ohsako, J. M. Zeigler, and R. M. Hochstrasser, *Chem. Phys. Lett.* **162**, 455 (1989); J. R. G. Thorne, S. T. Repinec, S. A. Abrash, and R. M. Hochstrasser, *Chem. Phys.* **146**, 315 (1990).
- ²⁰*Langmuir-Blodgett Films*, edited by G. Roberts (Plenum, New York, 1990); M. Orrit and P. Kottis, *Adv. Chem. Phys.* **74**, 1 (1988).
- ²¹D. Mobius and H. Kuhn, *Isr. J. Chem.* **18**, 375 (1979); D. Mobius and H. Kuhn, *J. Appl. Phys.* **64**, 5138 (1988); F. F. So, S. R. Forrest, Y. Q. Shi, and W. H. Steier, *Appl. Phys. Lett.* **56**, 674 (1990).
- ²²J. R. Kuklinski and S. Mukamel, *Phys. Rev. B* **42**, 2959 (1990).
- ²³H. A. Lorentz, *The Theory of Electrons* (Dover, New York, 1952).
- ²⁴J. J. Hopfield, *Phys. Rev.* **182**, 945 (1969); U. Fanó, *ibid.* **103**, 1202 (1956).
- ²⁵H. Haken and Y. Strobl, *Z. Phys.* **262**, 135 (1973).
- ²⁶S. Schmitt-Rink, D. A. B. Miller, and D. S. Chemla, *Phys. Rev. B* **35**, 8113 (1987); S. Schmitt-Rink, D. S. Chemla, and H. Haug, *ibid.* **37**, 941 (1988).